KU LEUVEN

FACULTY OF SCIENCE

Functional and anatomical characterization of neuropeptidergic signalling in PVQ neurons of *C. elegans*

Greeshma Soorambail

Supervisor: Prof. William A. Schafer
Animal physiology and Neurobiology

Co-supervisor: Prof. Isabel Beets
Animal physiology and Neurobiology

Mentor:

Jun Meng
Animal physiology and Neurobiology

Lidia Ripoll-Sánchez
MRC Laboratory of Molecular Biology, Cambridge

Thesis presented in

fulfillment of the requirements

for the degree of Master of Science

in Biophysics, Biochemistry and Biotechnology

Academic year 2023-2024

Host lab information page.

Master theses performed in the Schafer/Beets lab comply with following house rules:

1. *Maximal education and scientific self-empowerment of students*

   Students are encouraged to learn from their mistakes through dialogue, rather than by simply being corrected by their supervisors. All writing in this document is the result of this process.

   Students get two feedback moments with respect to their writing process. One from their daily supervisor, who will advise them on format and content (*e.g.* scientific language, proper representation of results and structure of their interpretations). For this, daily supervisors interact either in person with the student, or via comments added to the manuscript. Under no circumstances do they rephrase sections of the text, which is entirely the student's wording. A second feedback session includes comments from (co)supervisors and only focuses on content. This implies additional input with regards to the student's findings and the final discussion of results. The student's interpretation of this feedback is integrated in the final version of this manuscript, as it is presented here.

2. *Authenticity in science*

   Potential plagiarism was verified using TurnItIn. This work overall scored 14% of potential plagiarism. Sections underlying this result were manually verified by the daily supervisor, as such supporting the authenticity of this work.

   We encourage responsible use of writing assistance, including AI language models. The text in this document was produced with language support of ChatGPT.

Acknowledgments

I would like to express my sincere gratitude to my daily mentors, Jun Meng and Lidia Ripoll-Sánchez, for their invaluable guidance, patience, and unwavering support throughout this journey. Their expertise and support have been instrumental in this journey!

I am deeply thankful to my supervisor, William Schafer, for his patient mentorship, insightful feedback, and continuous engagement. I am also thankful to my co-supervisor, Isabel Beets, for her calming guidance and constructive criticism.

I would like to thank my family for their unwavering love, support, and understanding throughout this journey. They have been my source of strength and motivation.

I am also grateful to my fellow master's thesis students in the worm lab for their camaraderie. Special thanks to my friends for their support and encouragement throughout this process.

Lastly, I would like to extend my sincere thanks to the readers of my thesis, Prof. Liliane Schoofs and Dr. Jan Watteyne, for their time, expertise, and evaluation.

Contribution Statement

The conception and design of this work were executed under the invaluable guidance of my daily mentors, Lidia Ripoll-Sánchez and Jun Meng, with the oversight and approval of my promoter, William Schafer, and co-promoter, Isabel Beets.

For the execution of specialized procedures involving sophisticated machinery, Jun Meng conducted the microinjection for strain generation and capturing images through confocal microscopy.

The annotation and segmentation of the EM dataset was carried out by me. Subsequently, the segmentation data was rendered into a 3D image through the use of computer program, Autodesk 3ds Max, carried out by Lidia Ripoll-Sánchez.

Table of Contents

Abbreviations

CATMAID	Collaborative Annotation Toolkit for Massive Amounts of Imaging Data
CCK	Cholecystokinin
C. elegans	*Caenorhabditis elegans*
DCVs	Dense-Core Vesicles
DMSO	Dimethylsulfoxide
E. coli	*Escherichia coli*
EM	Electron Microscopy
ER	Endoplasmic Reticulum
GFP	Green Fluorescent Protein
GPCR	G-protein-coupled receptor
KI	Knock-in
KO	Knock-out
LB	Lysogeny Broth
NGM	Nematode Growth Medium
NLP	Neuropeptide-like Proteins
PCR	Polymerase Chain Reaction
PNs	Projection Neurons
RIP	Ring Interneurons
SVs	Synaptic Vesicles
VAST	Volume Annotation and Segmentation Tool
VNC	Ventral Nerve Cord

Scientific summary

Connections between neurons in the brain form a framework that enables neuronal communication. This map of neuronal connections is known as a connectome, which can be either "wired," involving synaptic connections, or "wireless," involving extrasynaptic volume transmission. Significant neuronal interactions occur through volume transmission, where neuromodulatory molecules released extrasynaptically activate receptors on neurons that are not synaptically connected and may be located distantly. However, compared to the wired connectome, there are fewer studies investigating the anatomy and function of the wireless connectome in animal brains.

In this study, the anatomy and behavioural role of extrasynaptic neuropeptidergic signalling were characterized in highly peptidergic neurons using the model organism *C. elegans*. Based on previous research from our lab, the PVQ class of neurons was chosen as an example of highly peptidergic neurons. A two-pronged approach was employed, involving the investigation of the functional significance of peptidergic signalling and the anatomical localization of neuropeptide-carrying vesicles in PVQ neurons.

It was found that disrupting peptidergic signalling in PVQ neurons significantly reduced the rate of forward locomotion in *C. elegans*, suggesting that peptidergic signalling is essential for normal locomotion. Additionally, neuropeptide-carrying vesicles, known as dense-core vesicles (DCVs), were abundant in PVQ neurons, particularly in the nerve ring region, which is considered the "brain" of *C. elegans*, implying that PVQ neurons are anatomically specialized for neuropeptide signalling. Additionally, a strain was designed that allows visualization of neuropeptide-carrying DCVs using fluorescent labelling of a DCV-marker protein, IDA-1.

Future research could investigate candidate neuropeptides, such as FLP-16 and NLP-13, expressed by PVQ neurons for their role in controlling locomotion. Other potential behavioural functions of peptidergic signalling, such as oxygen sensing, could also be explored. Additionally, studying the distribution of synapses and the presence of DCVs in these regions, through EM images, might provide insights into the mechanism behind DCV release in this area. Finally, by visualizing and observing the movement of DCVs, the fluorescently labelled IDA-1 strain could be used to study the variation of DCV dynamics across different neuronal populations.

General-audience summary

Understanding how the brain processes information and controls behaviour is one of the biggest challenges in modern science. Neurons, the brain's communication cells, use two main methods to send signals to each other: direct physical connections, referred to as wired communication, and indirect, diffusion-based connections, referred to as wireless communication. My research focuses on the "wireless" method using signalling molecules called neuropeptides.

In this study, I used a small nematode worm called *C. elegans*, to study wireless signalling in the nervous system. Specifically, I looked at a pair of neurons called PVQ neurons. These neurons are rich in neuropeptides, even though they don't have many direct physical connections with other neurons. This made them an interesting subject for studying wireless neuronal communication.

My research found that when the neuropeptide signalling in PVQ neurons is disrupted, the worms showed unusual behaviour when moving forward. This suggests that neuropeptides are important for controlling forward movement in *C. elegans*. I also found that PVQ neurons have many tiny vesicles that carry neuropeptides, especially in the nerve ring, which is considered the worm's brain. This suggests that PVQ neurons are anatomically specialized for neuropeptide/wireless signalling. Finally, we created a special strain of worms that allows us to visualize these vesicles using a fluorescent tag.

These findings are important because they show that even neurons with few wired connections can play a significant role in controlling behaviour through neuropeptide signalling. This could help us understand more about how brains work.

Future research could investigate specific neuropeptides, like FLP-16 and NLP-13, produced by PVQ neurons to see how they affect worm locomotion. Other possible roles of neuropeptide signalling, like oxygen sensing, could also be explored. Additionally, by studying where synapses and DCVs are located using electron microscope images, we might understand how these vesicles release their contents. Finally, by watching the movement of these fluorescently labelled vesicles in real-time, we can learn how their behaviour varies in different types of neurons.

Introduction

1. An introduction to connectomics

A central goal of connectomics and of modern neuroscience is to understand how neuronal connectivity and communication shape animal behaviour (Ripoll-Sánchez et al., 2023; Scheffer et al., 2020). Connectomics involves mapping all neuronal connections within the brain. These connections can occur at physical contact points known as synapses (White et al., 1986a) or through extrasynaptic volume transmission (Luigi F. Agnati et al., 1992), which are referred to as the wired and wireless connectomes, respectively.

Connectomics employs computer-assisted, high-throughput techniques for image acquisition and analysis to structurally map neural circuits. With a connectome, neuroscientists aim to explore how the functional aspects of the nervous system arise from its structural architecture (Galili et al., 2022).

The wired connectome provides an anatomical blueprint of neuronal communication, involving detailed, high-density mapping of point-to-point connections between neurons at synapses (Beyer et al., 2022; Briggman & Bock, 2012; Galili et al., 2022). Current efforts focus on creating detailed maps of the wired connectome in various species, from the small nematode *Caenorhabditis elegans* to animals with complex organisms like fruit flies, mice, and humans (Winding et al., 2023; Witvliet et al., 2021; Scheffer et al., 2020; Verasztó et al., 2020; Cook et al., 2019; Oh et al., 2014; Van Essen et al., 2013).

In addition to synaptic connectomes, neurons can communicate "wirelessly" outside of synapses through the volume transmission of neuromodulatory molecules such as monoamines and neuropeptides (Fuxe et al., 2012; Trueta & De-Miguel, 2012a; Agnati, Fuxe, et al., 1986). Exploring the mechanisms of extrasynaptic volume transmission can therefore provide a more complete understanding of neuronal communication, complementing the study of wired connectomics.

This thesis aims to characterize extrasynaptic neuropeptidergic signaling between neurons using the nematode worm *Caenorhabditis elegans* (*C. elegans*) as a model organism. The focus is on the PVQ class of neurons, which is used as an example of a highly neuropeptidergic.

2. *C. elegans* is an excellent model system for neurobiology

Caenorhabditis elegans is an excellent model system for studying neurobiology and behaviour (Sengupta & Samuel, 2009). This small, free-living nematode worm is found in rotting fruit and plant material, in temperate climates (Sudhaus & Kiontke, 1996). Typically, *C. elegans* is a diploid hermaphrodite, but about 0.2% of progeny are male due to the spontaneous loss of one sex chromosome (Herman, 2005). *C. elegans* has

been extensively used as a model organism, initially for research in neurodevelopment (Brenner, 1974a).

C. elegans was the first animal to have its entire synaptic connectome mapped. Its compact nervous system consists of 302 neurons in the adult hermaphrodite (White et al., 1986a). Despite the small number of neurons, *C. elegans* exhibits a wide range of behaviours, including sensory and navigatory behaviours like chemotaxis and thigmotaxis, as well as learning and memory capabilities (Suzuki et al., 2008; Bargmann, 2006; Zhang et al., 2005). Moreover, a hermaphrodite adult can produce 300 nearly isogenic progeny, which helps control for genetic variation—a crucial factor when selecting a behavioural model, as behavioural traits are often highly multigenic (McDiarmid et al., 2018; Fisher R., 1919).

C. elegans is relatively easy to culture in the laboratory. It can be grown on agar plates with a lawn of bacteria (OP50, an E. coli strain) as food, and it has a short development period of 3 days at 20°C (this varies with temperature) (Stiernagle, 2006a; J. Sulston & Hodgkin, 1988; Vanfleteren, 1980). Additionally, *C. elegans* is transparent, allowing for easy labelling and visualization of cellular and sub-cellular structures using fluorescent markers (Chew et al., 2018; Maulik et al., 2017). These factors make *C. elegans* an ideal model for studying the mechanisms and functions of neuropeptidergic signalling.

3. The wired connectome of *C. elegans* can be mapped using electron microscopy

In the wired connectome, communication between neurons occurs through synapses, which may be chemical or electrical. Chemical synapses involve transmission of a signal by the release of neurotransmitters in the synaptic cleft (Bernardo S. & Morgan S., 2012) whereas electrical synapses refer to transmission of a signal through intercellular channels called gap junctions (Bennett & Zukin, 2004).

C. elegans is the first animal to have its complete connectome mapped. This was carried out by the Brenner lab in the 1980s by reconstructing images obtained from electron microscopy (EM) of nervous tissue sections. EM images of synaptic-level resolution were captured from serially cut, ultrathin tissue layers (≈ 50 nm); followed by reconstruction and segmentation of the images (White et al., 1986a). The whole study took around a decade to be complete.

However, technological advances, such as high-pressure freezing for sample fixation, better contrast techniques, automation of tissue sectioning, and digitization of electron microscopy images (Mulcahy et al., 2018; Rostaing et al., 2004), and advances in computation technology, such as automated machine learning, image acquisition and analysis and 3D reconstruction software, is making it easier and faster to develop detailed maps of synaptic neural circuits (Mulcahy et al., 2018; M. Xu et al., 2013; Cardona et al., 2012).

To understand the behaviour of an animal, it's important to have an anatomical model of the structures that drive its behaviour (Cook et al., 2020, 2019). For this, a connectome generally includes synaptic-resolution level of information for each neuron, including its physical contact points to other neurons (synaptic partners). For instance, in a study of the posterior nervous system of an adult male worm, a wiring diagram was developed for synaptic connectivity in tail ganglia region. Network analysis of this diagram revealed the anatomical structures of a decision-making circuit that governs mating behaviour in males (Jarrell et al., 2012).

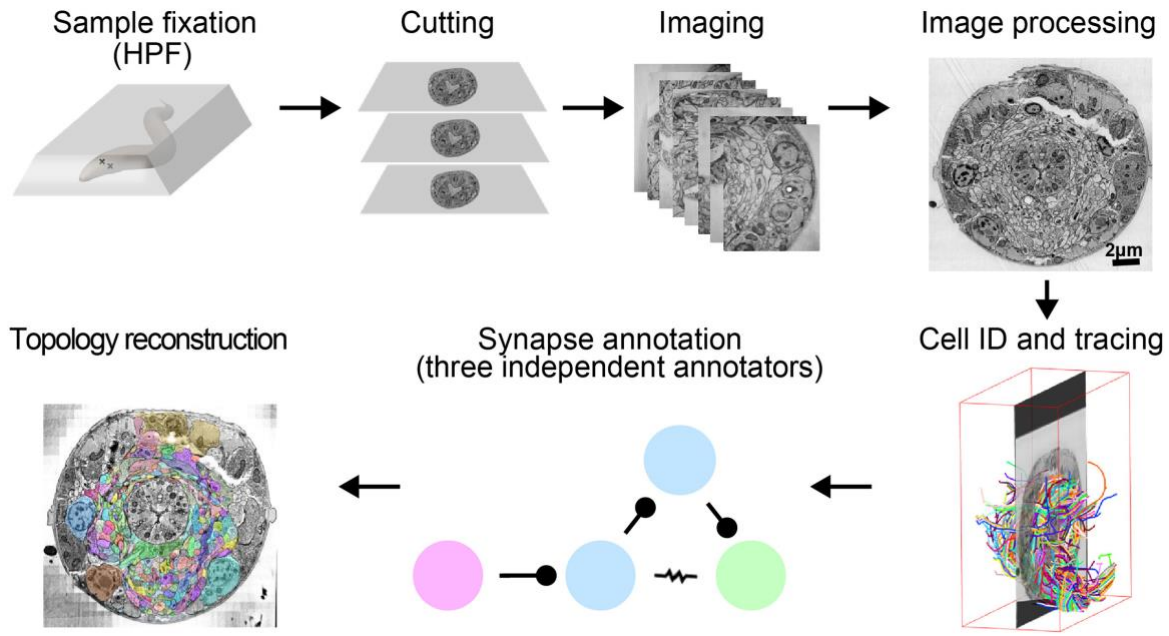

Figure 1. General workflow for connectome reconstruction using electron microscopy (Figure 1, Mulcahy et al., 2018)**.** The general electron microscopy workflow involves three main steps: sample preparation, imaging, and analysis. In 2018, the Zhen lab developed a pipeline for volume electron microscopy for the nervous system of *C. elegans*. The samples were fixed using high-pressure freezing and embedded in resin. The embedded sample was cut into ultra-thin sections and imaged on an electron microscope. These images were then stitched together and aligned into a 3D volume reconstruction. The neurons were identified based on the position of their cell body, the placement and trajectory of its neurites and its associated stereotypical structures and connectivity patterns. For this purpose, the software, CATMAID (Saalfeld et al., 2009a) and VAST (Berger et al., 2018) was used. To minimize subjectivity, the dataset was annotated for chemical and electrical synapses by three independent annotators.

3.1. The limitations of wired connectomics

The wired connectome reflects the anatomical structure of physical contact points between neurons. However, information on synaptic connectivity alone does not

capture the functional connectivity of neurons, and thus, cannot alone be used to predict behaviour (Randi et al., 2023).

The wired connectome forms a structural framework through which neurons can communicate; however, the connectivity and activity of neurons is very dynamic, modulated by several neuromodulatory molecules, such as monoamines, neuropeptides and neurohormones (Lee & Dan, 2012a; Marder, 2012a; Beverly et al., 2011).

In addition to this, neuromodulatory molecules also form an extrasynaptic signalling network for neuronal communication. These molecules can be released from non-synaptic sites, diffuse through the extracellular matrix, and can act over longer distances and over longer timeframes. Therefore, to study neuronal communication, wired connectomics alone is not sufficient (Luigi F. Agnati et al., 1992; Trueta & De-Miguel, 2012a).

Besides this, several mechanisms contribute to the dynamic nature of neuronal communication. For instance, connectomes developed from EMs images lack information on the type of neurotransmitters and neuromodulators released, presence of neuropeptidergic autocrine connections (for self-modulation), different post-synaptic receptors and their binding strengths and so on (Vogt, 2020). These factors add to the dynamicity of neuronal communication and function.

4. The wireless connectome of *C. elegans*

While the wired connectome represents the synaptic connectivity of neuroanatomy, the neuromodulatory signalling network elucidates the role of extrasynaptic volume transmission in neuronal communication.

In the mid- to late-20th century, increasing evidence indicated that neurons could communicate outside of synapses, through extracellular spaces (Fuxe et al., 2012; Trueta & De-Miguel, 2012a; Agnati, Fuxe, et al., 1986; Agnati, Zoli, et al., 1986). This evolved into a new theory of volume transmission in the brain that complemented conventional synaptic transmission, forming a more complete picture of how neurons communicate (Luigi F. Agnati et al., 1992). Volume transmission refers to the various signalling mechanisms in the nervous system that involves release of signalling molecules, such as neurotransmitters and neuromodulators, into extracellular medium. These molecules can diffuse across a relatively long-range, communicating with nearby and distant cells over a longer time frame (Trueta & De-Miguel, 2012b).

Neuromodulatory molecules, such as monoamines and neuropeptides, can modulate a diverse range of behaviour in animals, ranging from local action on individual neurons and small circuits to global brain networks affecting the behavioural state of an animal (Lee & Dan, 2012b; Liu et al., 2012; Marder, 2012b; Beverly et al., 2011; Marder & Bucher, 2007).

In *C. elegans,* monoamines and neuropeptides are associated with regulating several essential behaviours, including locomotion, reproduction, learning and feeding (Van

Damme et al., 2021; Watteyne et al., 2020; Chang et al., 2015; Chase & Koelle, 2007; Kawano et al., 2000; Li et al., 1999; Nelson et al., 1998). These molecules function by activating their cognate receptor which are generally G protein-coupled receptors (GPCRs). In the nervous system, some examples of monoamines include serotonin, dopamine, adrenaline (Swallow et al., 2016; Walker et al., 1996); and neuropeptides include vasopressin, oxytocin, cholecystokinin (CCK) (de Wied & van Ree, 1989; Heinrichs & Domes, 2008; Ye et al., 2019).

Neuropeptides are messenger molecules, made of short chains of amino acids, synthesized, and released from neurons (Mains & Eipper, 1999). There are over 300 neuropeptide molecules found in *C. elegans*, encoded by at least 159 genes. They are extensively expressed in the nervous system, with each neuron class expressing a distinct combination of neuropeptides (McKay et al., 2022; Taylor et al., 2021; Van Bael et al., 2018; Li & Kim, 2008).

Neuropeptides are derived from large precursor molecules that are cleaved and modified post-translationally (Li & Kim, 2008). The initial steps of processing the precursor molecules are carried out by a group of enzymes called the proprotein convertases. EGL-3 is an important proprotein convertase enzyme expressed in many neurons (Kass et al., 2001).

Previous studies have indicated that EGL-3 is a major protein involved in processing precursor molecules into neuropeptides that show diverse functions, including egg-laying, mechano-sensation, and locomotion (Husson et al., 2006; Jacob & Kaplan, 2003; Kass et al., 2001).

Processing of precursor molecules begins at the endoplasmic reticulum, then in the Golgi complex and continues as the peptides are packaged into dense-core vesicles (DCV) and trafficked across the axon, to nerve terminals (Mains & Eipper, 1999; Fleur L Strand, 1998).

4.1. The neuropeptidergic signalling network of *C. elegans*

It is widely accepted that neuropeptides might exert their effects beyond the location where they are initially released (Nässel, 2009). In a study of sympathetic ganglion in bullfrogs, it was demonstrated that neuropeptides once released, may diffuse over tens of micrometres to bind to their cognate receptors (Jan & Jan, 1982).

In addition, several studies have indicated that DCV cluster in perisynaptic and non-synaptic regions (Nässel, 2009; Nusbaum, 2002; Ohnuma et al., 2001; Karhunen et al., 2001). Conversely, synaptic vesicles (SVs) carrying classical neurotransmitters cluster at the active zone. The difference in positioning of SV and DCV may play a significant role in the different requirements for their release (Nusbaum, 2002; Karhunen et al., 2001).

For instance, in a study on the buccal neurons of *Aplysia californica,* it was observed that the exocytosis of DCV requires a higher stimulus frequency than for exocytosis of

SV. The released peptides bind to their cognate GPCRs, activating the second messenger cascade (Nässel, 2009; Karhunen et al., 2001). The range of action of secreted neuropeptide could be limited by dilution, binding affinity of the cognate receptor and by the activity of membrane-bound peptidases (Nässel, 2009; Ohnuma et al., 2001).

Neuropeptides are interesting to study as they are the most diverse class of neuromodulators found in the nervous system (Jékely et al., 2018). Generally, in bilaterian animals, the genome encodes hundreds of neuropeptides and GPCRs (Beets et al., 2023; Taylor et al., 2021b; Civelli et al., 2013; Mirabeau & Joly, 2013; Caers et al., 2012; Frooninckx et al., 2012). These genes are widely expressed across the nervous system. In comparison, the expression of monoamines is generally restricted to a small group of neurons (Bentley et al., 2016).

A recent study developed a draft connectome of neuropeptidergic signalling in *C. elegans,* based on information on neuroanatomy, single-cell expression dataset and neuropeptide-GPCR pairing (Beets et al., 2023; Ripoll-Sánchez et al., 2023; Taylor et al., 2021b). Neuropeptidergic signalling was found to be a dense, pervasive, and decentralized network, which has a topology distinct from the network topology of the synaptic connectome.

The neuropeptidergic signalling network of *C. elegans* exhibits a rich-club topology, a concept from network theory. This refers to a group of neurons, termed as nodes, that show the highest degree of connection with other neurons, are more densely interconnected amongst themselves than would be expected from their high degree alone. Notably, the rich club of *C. elegans* encompasses more than half of all its neurons, indicating a densely connected and decentralized neuropeptidergic connectome. However, some neurons exhibit exceptionally high degree of neuropeptidergic connections. These neurons are referred to as hubs, with their high degree being an indication of their functional significance.

The neuropeptidergic signalling network of *C. elegans* has 6 highest-degree hub neurons, which includes AVK, PVQ, PVT, and PVR (Ripoll-Sánchez et al., 2023). The neuron classes AVK and PVT are known to be peptidergic neurons and do not express any classical neurotransmitters and monoamines (Pereira et al., 2015). These neurons are associated with the modulation of arousal and sleep-like behavioural states (Niu et al., 2020; Oranth et al., 2018; Turek et al., 2016; Y. Xu et al., 2021).

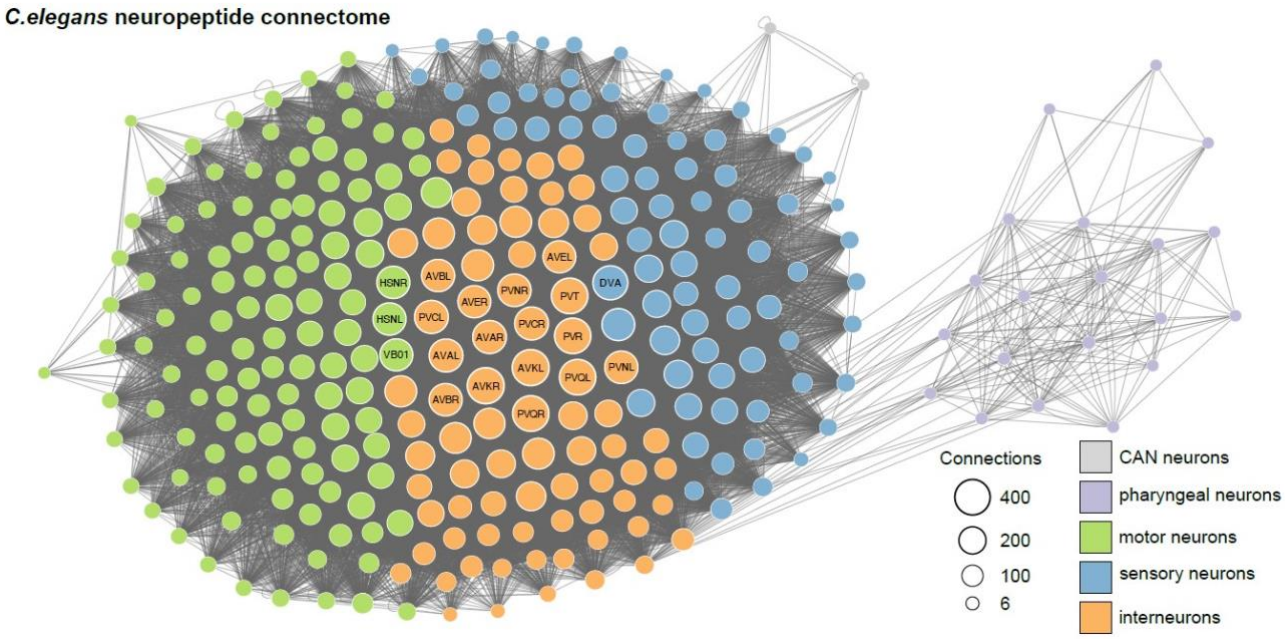

Figure 2. A graphical representation of the draft neuropeptidergic connectome of *C. elegans* (Figure 1, Ripoll-Sánchez et al., 2023)**.** The neuropeptide connectome was developed by integrating information from neuropeptide-GPCR pairing, single-cell gene expression, and anatomical datasets to infer potential pathways for neuropeptide signaling between individual *C. elegans* neurons. The neuropeptidergic signalling network was found to be a dense, pervasive, and decentralized network, which has a topology distinct from the network topology of the synaptic connectome.

PVQ and PVR neurons originate in the tail region and extend their processes to the nerve ring (White et al., 1986b). EM image analysis has revealed that their neuronal processes in the nerve ring are abundant with dense-core vesicles. This suggests a potential anatomical specialization for neuropeptidergic signalling, though their specific functions remain poorly understood (Ripoll-Sánchez et al., 2023; Witvliet et al., 2021). Furthermore, a recent study by Wang et al. found that PVQ neurons do not express classical neurotransmitters or monoamines (Wang et al., 2024b).

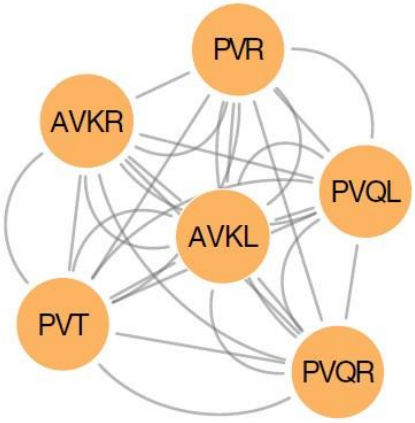

Figure 3. A representation of network connectivity between six highest-degree neuropeptidergic hub neurons in *C. elegans* (Graphical abstract, Ripoll-Sánchez et al., 2023)**.** The six highest-degree hub neurons in the neuropeptidergic signalling network of *C. elegans*. These are little-studies neurons that appear to be specialised for peptidergic signalling. AVKL/R, PVQL/R and PVT neurons are known to be peptidergic neurons that do not express any classical neurotransmitters and monoamines (Wang et al., 2024; Pereira et al., 2015). Meanwhile, PVR and PVQ neurons are known to be rich in DCVs (Ripoll-Sánchez et al., 2023; Witvliet et al., 2021).

5. The anatomy of the *C. elegans* nervous system

To investigate the dynamics of both wired and wireless connectomes, it is essential to understand the anatomical structure of the *C. elegans* nervous system. The organization and physical properties of neurons and their processes provide the foundation upon which both types of connectomes operate.

The *C. elegans* nervous system consists of a compact but organized structure, facilitating the study of both wired and wireless connectomes by providing a framework on which they function.

An adult hermaphrodite worm has nervous system consisting of two distinct and autonomous systems: a somatic nervous system which is comprised of 282 neurons and a pharyngeal nervous system with 20 neurons (White et al., 1986a; J. E. Sulston & Horvitz, 1977). The pharyngeal nervous system is synaptically connected to the somatic nervous system through a pair of neurons known as ring interneurons (RIP) (White et al., 1986a).

In comparison, the neuropeptidergic network forms several putative connections between the central and pharyngeal nervous system. Pharyngeal neurons express several GPCRs whose ligands are expressed by non-pharyngeal neurons, indicating that these neurons are peptidergically connected to non-pharyngeal neurons (Ripoll-Sánchez et al., 2023; Taylor et al., 2021b).

Neurons are grouped into 118 different classes based on their topology and synaptic connections (White et al., 1986a). Most neurons in *C. elegans* are unipolar or bipolar with very thin, unbranched processes. The cell-bodies of most neurons cluster together to form ganglia in the head or tail region. From theses ganglia, neuronal processes arise and run along in longitudinal nerve bundles, forming several chemical and electrical synapses (Hall et al., 2005; White et al., 1986a).

In regions with synapses, local swelling is observed, along with clusters of SVs and of DCVs in the active zone and the perisynaptic regions, respectively. DCV, similar to SV and other vesicles, undergo microtubule-dependent fast transport in neurons, facilitated by motor proteins belonging to the kinesin and dynein superfamilies (Rudolf et al., 2001; Tsukita & Ishikawa, 1980).

Neuronal processes (also known as neurites) contain bundles of microtubules, smooth endoplasmic reticulum and at times, clusters of free ribosomes (for local translation) and mitochondria (Rolls et al., 2002; White et al., 1986). Also, the nerve ring, present in the head region, has the largest collection of neurons in the worm body, while the tail ganglia region has the second largest neuron collection.

In *C. elegans*, neurons are classified into four categories based on their functional role: (1) motor neurons (make synaptic connections with muscle cells); (2) sensory neurons (detect and transmit sensory cues); (3) interneurons (connect motor neurons and sensory neurons); and (4) polymodal neurons (can perform multiple functions). Of these neuron types, interneuron is the largest group of neurons in *C. elegans*.

Interneurons receive incoming synapses from and transmit outgoing synapses to other neurons, functioning as information processors. They do so by coordinating information from various sensory neurons, possibly from different neuronal circuits, modulating the execution of a behavioural program. For example, the neuronal networks for egg-laying and locomotion are linked by the interneurons AVF, AVJ and AVB. These cells act as circuit couplers that can connect different circuits to temporally coordinate their activity (Hardaker et al., 2001).

Interestingly, the six highest neuropeptidergic hub neurons in *C. elegans* are all interneurons with long processes extending from the nerve ring to the tail region. This may indicate a morphological specialization of these neurons for local peptidergic release throughout the entire nervous system (Ripoll-Sánchez et al., 2023).

In this thesis, we focus on characterizing neuropeptidergic signalling in a specific class of neurons known as PVQ. As previously mentioned, PVQ consists of a pair of interneurons, PVQL and PVQR, born in the lumbar ganglia of the tail region. The neuronal processes of these two neurons extend along the ventral nerve cord of *C. elegans*, with PVQL extending along the left tract and PVQR along the right tract, reaching up to the nerve ring (White et al., 1986b). The functional role of PVQ neurons

remains insufficiently explored. However, PVQL, along with PVP neurons, appears to guide axons along the left tract during VNC development (Durbin, 1987).

In the draft neuropeptidergic connectome of *C. elegans* by Ripoll-Sánchez et al., PVQ neurons are anticipated to connect extensively with neurons in the URX, PQR, BAG, BDU, VB, and DB classes. These neurons are part of neural circuits responsible for oxygen sensing, forward movement, and proprioception, indicating a potential functional role for PVQ neurons in regulating these behaviours (Gray et al., 2004; Wen et al., 2012a; Zimmer et al., 2009).

Given the predicted connections of PVQ neurons with those involved in these behaviours, it is important to conduct behavioural assays targeting these specific behaviours. To this end, disrupting peptidergic signalling in PVQ neurons would enables us to investigate the role of neuropeptide-based signalling in locomotion, providing insights into how this signalling influences these behavioural processes in *C. elegans*.

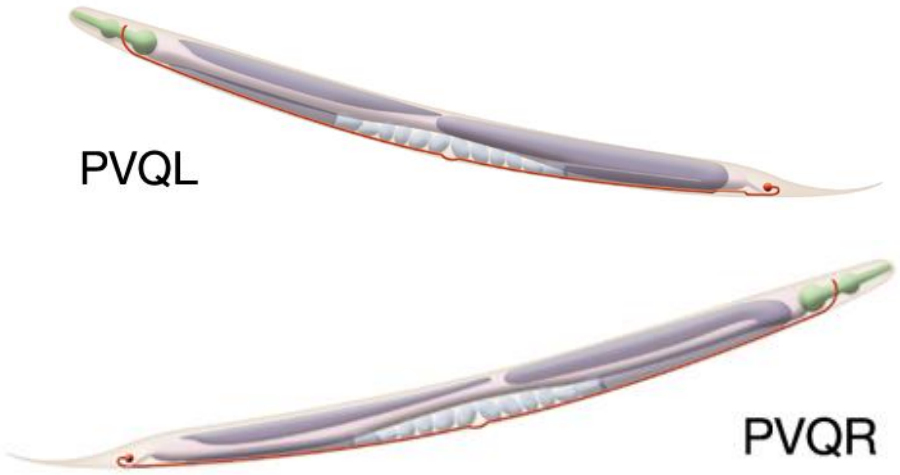

Figure 4. Placement and topology of PVQ neurons in the ventral nerve cord. PVQ is a class of interneurons in *C. elegans.* This class is comprised of two neurons, PVQL and PVQR, originating in the posterior or tail region of the worm. Their axons project anteriorly, along the ventral nerve cord up to the nerve ring (White et al., 1986b). PVQ neurons forms synaptic connections with ASJ, ASK and AIA neurons (Witvliet et al., 2021). Being neuropeptidergic hub neurons, PVQL/R forms several strong peptidergic connections, with the most significant associations observed with URX, PQR, DB and VB neurons (Ripoll-Sánchez et al., 2023).

6. Dense-core vesicles (DCVs) and neuropeptidergic signalling

The anatomy of the *C. elegans* nervous system is crucial for forming a structural framework for neuropeptidergic signaling. Within this framework, dense-core vesicles (DCVs) are components that mediate the storage, transportation, and release of neuropeptides, which are essential for wireless communication between neurons.

As mentioned previously, precursor neuropeptide molecules are packaged into DCV along with their processing enzymes (Introduction: Section 4.1.). This packing occurs at the trans-Golgi network, followed by trafficking of the vesicles along the axons. The release of DCV content, including neuropeptides, generally occurs at non-synaptic sites, contributing volume transmission (Salio et al., 2006; Strand, 1999).

In this manner, DCVs play an essential role in the operation of the neuropeptidergic signalling network. Witvliet et al. (2021) used serial-section electron microscopy to reconstruct the nerve ring region of *C. elegans* across its various developmental stages. It was observed that the neuronal processes of the PVQ class of neurons is abundant in DCVs in the nerve ring region. This is in consensus with the findings of Ripoll-Sánchez et al. (2023) that identified PVQ neurons as a neuropeptidergic hub.

Therefore, electron microscopy images of *C. elegans* nervous system can be used to localize DCVs in a neuron, revealing detailed morphological information and valuable quantitative data, including their number and distribution (Witvliet et al., 2021; White et al., 1986).

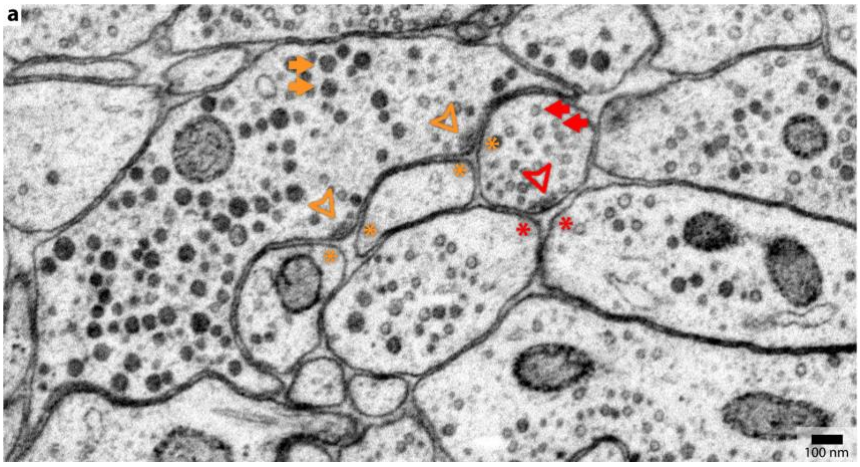

Figure 5. A representative electron microscopy image of neurons carrying DCV and SV (Extended Data Fig. 1) (Witvliet et al., 2021)**.** The pre-synaptic terminal with the classical chemical synapses is indicated by a red arrowhead. It is rich in SVs (red arrows), which are in the active zone. In contrast, the neuronal processes of modulatory neurons, like PVQ, are abundant in DCVs, highlighted by the orange arrows. These DCVs are also located in the pre-synaptic terminal but away from the

classical chemical synapse marked by an orange arrowhead. The postsynaptic neurons are denoted by an asterisk.

Most neuron classes in *C. elegans* are developed (birth, extension of their neuronal processes and forming synapses) during embryogenesis i.e. before hatching or the L1 stage. This includes PVQ neurons and all the connections they form (H. Sun & Hobert, 2023; H. S. Sun & Hobert, 2021; Witvliet et al., 2021). Certain classes of motor and sensory neurons are developed between the L1 and L3 larval stages, while most male-specific neurons are generated during the L3 and L4 larval stages (H. Sun & Hobert, 2023).

In addition to analyzing EM data, DCV localization can also be achieved by introducing a fluorescent tag on a marker protein within PVQ neurons (He et al., 2019). IDA-1, a transmembrane protein found in DCVs, is commonly used as a marker for visualizing these vesicles by fusing it with green fluorescent proteins (GFP) (Zahn et al., 2004). For instance, Valperga and de Bono (2022) tagged DCVs with IDA-1::GFP, expressed specifically in ADL neurons, to study the mechanism of cross-modal plasticity. After ADL neurons lost their sensory properties, their function was repurposed by the oxygen sensing circuit, leading to increased neuropeptide secretion by ADL neurons. This study examined whether this increased secretion was accompanied by heightened DCV trafficking in the neuron.

In this manner, DCVs can be visualized by fluorescently labelled DCVs in neurons. And expression of DCVs is indicative of peptidergic signalling activity in the neuron.

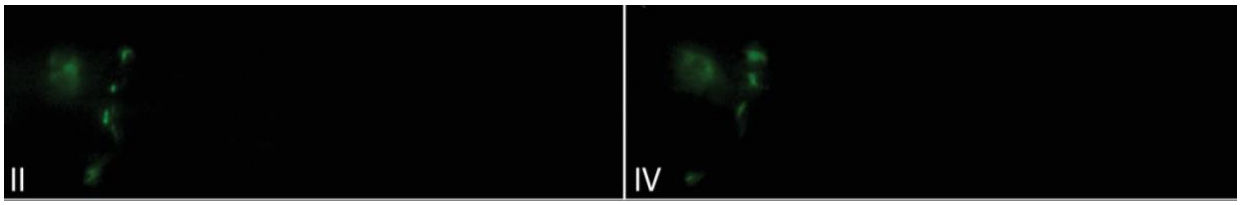

Figure 6. Localization of IDA-1::GFP in ADL neurons in wild-type animal and in *qui-1* mutant animal (Figure 3 – Figure supplement 1 (C), Valperga & de Bono, 2022)**.** In this study, the distribution and potential release sites of DCV was investigated by fluorescently tagging IDA-1 in ADL neurons. ADL comprises of two sensory neurons situated in the head region. These neurons exhibit a high degree of polarisation, with its one dendrite extending towards the nose and the axon moves posteriorly towards the nerve ring, bifurcating into two branches. The IDA-1::GFP fluorescence was observed as small, bright spots along the axon and more widely dispersed in the cell body. However, no fluorescence was detected in the dendrite.

Research Outline

A central goal of modern neuroscience is to understand how the brain processes internal and external information through neuronal circuits. Recent efforts have focused on mapping synaptic wiring diagrams, or synaptic connectomes, of both simple and complex nervous systems. However, neurons communicate through two distinct mechanisms: synaptic transmission via wired connections and volume transmission of neuromodulatory signalling molecules like monoamines and neuropeptides via wireless connections i.e. through extrasynaptic signalling.

To study extrasynaptic peptidergic signalling, we use *Caenorhabditis elegans* as a model organism. Ripoll-Sánchez et al. (2023) developed a draft neuropeptidergic connectome for *C. elegans*, revealing a dense and decentralized signalling network. Interestingly, the six neurons with the highest peptidergic connectivity did not exhibit high synaptic connectivity. This indicates that certain neurons are crucial in neuropeptide signalling despite limited synaptic connections.

Thus, this research investigates the functional and anatomical roles of neuropeptidergic signalling in PVQ neurons, a class of neurons that exhibits high peptidergic connectivity but low synaptic connectivity.

To disrupt peptidergic signaling in PVQ neurons, we aim to develop a PVQ-specific *egl-3* gene knockout strain. EGL-3 is necessary for the processing of neuropeptide precursors. By knocking out this gene, we aim to disrupt peptidergic signalling in PVQ neurons. Following the development of the knockout strain, we will characterize the functional role of peptidergic signaling in PVQ neurons through locomotion-based behavioral assays. These assays will allow us to observe the direct effects of disrupted peptidergic signaling on neuronal function and behaviour.

Additionally, we will also characterize the anatomical distribution patterns of neuropeptide-carrying dense-core vesicles (DCVs) in EM images. The images will be annotated and analyzed for DCVs in PVQ neurons. These images are obtained from L1-L2 transition stage larval worms. Therefore, the data is only representative of DCV distribution in a particular worm developmental stage.

To overcome the limitation of the EM dataset, we want to develop a strain that allows visualization of DCVs in real-time across various stages of the worm life cycle. We want to design a knock-in strain wherein a DCV marker protein, IDA-1, is fluorescently tagged in a cell-specific and endogenous manner. Visualization of DCVs will enable us to study the dynamics of neuropeptidergic signalling, providing a more comprehensive understanding of DCV dynamics and spatial distribution throughout different developmental stages.

Materials and Methods

1. *C. elegans* maintenance and handling

1.1. *C. elegans* strains

All the strains used in this thesis project are listed in Table 1. These strains have an N2 background.

Table 1. List of *C. elegans* strains used in this research project.

Name	Strain	Genotype
Wild type	Bristol	N2
egl-3 floxed	DCR6978	*egl-3* (nu1711) V
PVQ-specific *egl-3* knockout [*nlp-17p*(296 bp)]	IBE815	*egl-3* (nu1711) V; ibtEx143 [*nlp-17p*(296 bp)::CRE (20 ng/uL) + *unc122*p::GFP (50 ng/uL)]
IDA1	PHX9058 (AQ5368)	LoxP-ida-1(exon-12)-LoxP-ida-1 3' UTR-mNeonGreen

1.2. Culturing conditions

All *C. elegans* strains utilized in this research project were maintained on nematode growth medium (NGM) plates that were seeded with bacteria, *E. coli* OP50, as the food source, at 20°C (Brenner, 1974). All the strains were raised under identical conditions.

1.2.1. Preparation of Nematode Growth Medium (NGM) plates

The strains were maintained on medium sized (55mm) plates, containing 12mL of the Nematode Growth Medium (NGM) agar prepared according to the standard protocol (Brenner, 1974; Stiernagle, 2006). Once prepared, the plates were inverted and stored at 4°C.

1.2.2. Seeding of Nematode Growth Medium plates

An *E. coli* OP50 overnight culture was prepared by inoculating 10mL of Lysogeny Broth (LB) medium with a colony of *E. coli* OP50. The NGM agar plates were seeded with 100µL of the *E. coli* OP50 culture medium and then left to dry. Once dried, the closed plates were inverted and kept at room temperature overnight, allowing the seeded bacteria to grow. The next morning, plates were ready to be used or stored at 4°C until needed.

1.2.3. Propagation of *C. elegans* hermaphrodites for strain maintenance

Regular maintenance of *C. elegans* strains was carried out by transferring three young adult hermaphrodite worms to NGM agar plates with a fresh OP50 lawn. This was

carried out every 3-4 days when kept at 20°C. Since *C. elegans* can grow and multiply very rapidly, it is important to transfer worms to new plates as otherwise the bacterial lawn would be depleted, and the worms would be starved, and this can change their behaviour. Generally, the worms were transferred by picking/scooping up the worm with a worm picker.

1.3. Freezing *C. elegans* strain

C. elegans strains can be frozen and stored for an indefinite period. These strains can be then recovered for use, by thawing. This allows strains to be stored and acts as a backup stock for use in the future. Freezing is ideally carried out on worms that are in the L1-L2 transition state, from a freshly starved plate (these worms survive freezing best). The standard protocol for freezing was followed (Brenner, 1974; Stiernagle, 2006).

2. Molecular biology techniques

2.1. Assembly of promoter-Cre recombinase construct

Linearizing vector pJH4237

For assembly of the promoter-Cre recombinase construct (for the PVQ-specific *egl-3* knockout strain), the plasmid vector pJH4237 (*Ptwk-40s*::Cre unc-54 3' UTR C.elegans for Cre/Lox) was obtained for use from the Zhen lab (Lu et al., 2022). The structure of the plasmid vector is provided in the Appendix section. The vector was linearized with the restriction enzymes, SphI and SmaI (FastDigest, Thermo Fischer Scientific) flanking the original promoter sequence of the plasmid. The restriction digestion mix was prepared by adding the components mentioned in table 3. And then incubating at 37°C for 60 minutes. The resulting DNA fragments were visualized through gel electrophoresis.

Table 3: Reaction components used in the restriction-digestion mix.

Component	Concentration	Volume
Plasmid DNA	97.65ng/ µL	10µL
10x FastDigest Buffer		3µL
Restriction enzyme		1µL/enzyme
PCR-grade water		15µL

For the gel electrophoresis, a gel containing 1% agarose (Sigma-Aldrich) was prepared with 5µL of GelRed (10000x in Dimethylsulfoxide (DMSO), Biotium) for visualization of DNA. The gel was run for 50 minutes at 110V and then visualized under UV light. The correct band length (4543 bp) for the vector construct without the original promoter (*Ptwk-40*) was extracted from the gel using the Zymoclean Gel DNA Recovery Kit.

Cloning genomic DNA

The DNA sequence for the promoter of *nlp-17* gene (298bp) was obtained from the Frøkjær-Jensen Lab (DNA sequence given in the Appendix section) (AlHarbi & Frøkjær-Jensen, 2023). This DNA fragment was amplified from the genomic DNA of *C. elegans* by polymerase chain reaction (PCR). For successful DNA assembly, the primers have an overhanging sequence that is complementary to the overhanging sequence of the linearized vector, facilitating the annealing and assembly of the DNA fragments. The primers used here are given in Table 4.

Table 4. A list of the primers used for the PCR amplification of nlp-17 promoter with their sequence and annealing temperature.

Primer	Sequence	Annealing Temperature
PJM1558 (forward)	CCATGATTACGCCAAGCTTGCATGCACTTTGATGTTTCAAAAGTTTTCCT	62°C
PJM1559 (reverse)	CTTTGGGTCCTTTGGCCAATCCCGGGTCTGTGAAAAAGCCTGACTTT	62°C

A 50µL PCR master mix was prepared and then placed in a thermocycler (Mastercycler nexus gradient, Eppendorf) and run with the PCR program mentioned on Table 5. This was followed by visualization and extraction of the amplified DNA fragments by gel electrophoresis and gel extraction of the sample, respectively.

Table 5. PCR program used for Q5® High-Fidelity DNA Polymerase.

Phase	Temperature	Duration
Initial denaturation	98°C	30 seconds
Denaturation	98°C	10 seconds
Hybridisation	62°C (annealing temperature)	30 seconds
Extension	72°C	30 seconds/kb
35 cycles		
Final extension	72°C	2 minutes
Hold	4°C	Pause

DNA fragment assembly

The NEBuilder HiFi DNA Assembly Cloning Kit was used as a one-step method for assembly of DNA fragments, under isothermal conditions. For a two-fragment assembly, a 1:2 concentration ratio of vector:insert is recommended. In a 1.5mL Eppendorf tube, kept on ice, 2µL of linearized vector, 4µL of promoter insert and 10µL of NEBuilder HiFi DNA Assembly Master Mix was added. Then, the total volume of the reaction mixture solution was brought to 20µL by the addition of PCR-grade water. The reaction mixture was incubated at 50°C for 60 minutes in a dry bath (Compact dry bath S, Thermo Fisher Scientific). The assembled product was then stored at -20°C.

The assembled plasmid vector was introduced into DH5 a competent bacterial cell through chemical transformation, following the standard protocol of Green and Sambrook (Green & Sambrook, 2012).

Diagnostic digest

To ensure that the cloning of insert into the vector was carried out successfully, a diagnostic digest was carried out. First, the plasmid vector was extracted from an overnight culture by following the protocol from the QIAprep Spin Miniprep Kit (Qiagen, Germany). Around 600 ng of plasmid DNA was digested with XbaI restriction enzyme, at 37°C, for 60 minutes. The digested product was separated by 1% agarose gel electrophoresis to confirm the presence of fragments at the correct band length, indicating the successful insertion of the promoter sequence into the vector.

3. Generation of egl-3 knockout in PVQ neurons

3.1. Preparation for microinjection

Preparation of injection mix

To prepare the injection mix, the reagents mentioned in Table 5 were added into a 1.5mL Eppendorf tube. The co-injection marker used had the genotype *unc122*p::GFP.

Preparation of Injection Pads

To ensure that the worms are immobilized during the microinjection, a 2% agarose injection pad was prepared according to the standard protocols (Kadandale et al., 2009).

Table 5: Description of the volumes and stock concentrations of the injection mix.

Component	Concentration	Volume (Total = 6µL)
Co-injection marker (*unc122*p::GFP)	50ng/µL	0.59µL

Cre-construct carrying plasmid	20ng/µL	0.38µL
RT-PCR grade water	-	5.03µL

3.2. Microinjection

For the microinjection, 30-40 L4 hermaphrodite worms were picked on to two plates in the afternoon of the day before the injection. One plate was placed at 16°C, while the other plate was placed at 20°C overnight. On the following day, the plate with plenty of young adult worms at the right stage was chosen for injection.

The microinjections were done by my daily mentor, Jun Meng. The injection was carried out on the cytoplasm of the gonadal syncytium. Once injected, the worms were placed onto a new seeded NGM plate, and kept in the incubator at 20°C. Once the worms recovered from the injection procedure, eggs were laid (F1 progeny). This was carried out on worms belonging two strains, DCR6978 (egl-3 floxed strain, to generate PVQ-specific *egl-3* knock-out worms) and PHX9058 (IDA-1 knock-in strain, to generate a PVQ-specific labelling of DCVs).

3.3. Confocal microscopy for strain validation

Capturing the images through confocal microscopy were done by my daily mentor, Jun Meng. These images were acquired using a Zeiss airy scan confocal and image stacks generated using Fiji. Worms, in L4 stage, were prepared for imaging by immobilizing them between two microscope coverslips with a dry pad for immobilizing the worm, allowing for high-resolution imaging.

4. Behavioural analysis

4.1. Preparation for recording of spontaneous locomotion

The day before the recording, 8-10 L4 worms in a similar developmental stage were transferred onto a new seeded plate in the afternoon. Four to five such plates were incubated at 20°C overnight. The day after, the day one adult worms were used for recordings of their spontaneous locomotion, carried out in the morning.

4.2. Spontaneous locomotion recording

On the day of the recording, unseeded NGM agar plates (55mm) with an essence of *E. coli* OP50 at the centre were used. These plates were prepared by placing a bit of OP50 bacteria, picked from a seeded plate, at the centre. The plates were allowed to rest for five minutes and then the OP50 bacteria was cleaned up using a glass Pasteur pipette that was bent around the pointed edge (with heat). This was done to ensure that the worms remain closer to the centre during the recordings.

Recording of spontaneous locomotion

At least thirty young adult hermaphrodite worms were recorded per genotype per day. In every NGM plate, five worms were placed for recording, followed by a 2-minute

habituation period. Then, the locomotion of the worms was recorded for 5 minutes, during the roaming state. The roaming state refers to an exploratory behavioural state characterized by long, straight, and continuous movements with fewer turns and changes in direction (Fujiwara et al., 2002). This was followed by recording of locomotion for the dwelling state for the next 10 minutes. The recordings were carried out under the Dino-Lite Edge digital microscope. The frame rate of the camera was set to 10 frames per second, which is ideal for behavioural analysis using the tracking software, TierPsy (Javer et al., 2018).

Table 4. List of strains used for recording of spontaneous locomotion.

N2 bristol	***I***	Wild type
egl-3 floxed	DCR6978	Negative control
PVQ-specific *egl-3* knockout [*nlp-17p*(296 bp)]	IBE815	Experimental group

4.3. Preliminary behavioural analysis

Quantification of locomotion rate

The recordings for the roaming state, each lasting 5 minutes, were analysed by measuring the locomotion rate through counting the body bends of 10 worms. Each body bend was counted when the part of the worm just behind the pharynx reached a maximum bend in the opposite direction from the previous counted bend. However, if the worm moved forward, then reversed direction spontaneously, and the same region behind the pharynx bent in the same direction as it had during the forward movement, this bend was not counted. The average body bends per minute were calculated by adding up the body bends counted for each worm over the entire 5-minute period and then dividing by 5. An unpaired t-test was used to determine the significance of the data.

Quantification of spontaneous reversals

Reversal behaviour describes the worms' tendency to switch their movement from forward to backward by altering the direction of their sinusoidal body waves. In the recorded data, 10 worms were observed to count the number of spontaneous reversals. A reversal was defined as any backward movement exceeding the length of the pharynx. The collected data was then analysed for statistical significance using an unpaired t-test.

5. Annotation of DCV in EM images

5.1. EM dataset features

The EM dataset used in this study were obtained from the Mei Zhen Lab (Mulcahy et al., 2018; Witvliet et al., 2021). The Zhen lab developed eight electron microscopy

volumes of wild-type (N2 strain) hermaphrodite worms, at different stages of their development, from birth to adulthood. In this research project, EM images obtained from the late L1 larval stage (16 hours after hatching) was used for DCV annotations. This was the oldest developmental stage vEM dataset available for the whole organism. Many neurons are fully formed in the embryonic stage, i.e. before hatching, followed by some other neurons classes that are born during the L1 stage, forming a representation of around 90% of the nervous system. Therefore, PVQ class of neurons and all their connections were assumed to be completely developed according to our knowledge (H. Sun & Hobert, 2023; H. S. Sun & Hobert, 2021; Witvliet et al., 2021).

The EM data set was developed by the Zhen lab (Mulcahy et al., 2018; Witvliet et al., 2021). The Zhen lab used isogenic worms reared in the same environmental conditions. The worms were prepared for microscopy through high-pressure freezing, followed by slicing the sample into serial sections of 30nm thickness. The images were acquired using ATUM-SEM at a resolution of 1 x 1 x 30nm. The images were stitched and aligned into a 3D volume using the software TrakEM2. For reconstruction of neurons, skeleton segmentation was carried out, wherein, neurons were identified and traced while placing a dot, known as a node, in the center of the neurite in each section. This was carried out with the software CATMAID (Collaborative Annotation Toolkit for Massive Amounts of Imaging Data) (Saalfeld et al., 2009b). The neurons were identified and reconstructed based on the cell body position and morphology.

5.2. Annotation of DCVs using Volume Annotation and Segmentation Tool (VAST)

Volume annotation and segmentation tool (VAST) is a software tool used for generating and editing annotations and segmentations of large 3D image datasets. This tool can be used for segmentation of intracellular ultrastructure such as the Golgi apparatus, endoplasmic reticulum (ER), synapses, and even dense core vesicles (DCVs). Therefore, valuable biological information related to their morphology, size, number, and distribution can be obtained from this type of data.

Identifying and annotating DCV:

The neurons annotated for this experiment are given in Table 6. A complete neuron was traced for DCVs by moving across the slides of the image stack, using the skeleton nodes of the neuron as a reference. For each neuron, the DCVs present in different regions of the neuron, i.e. nerve ring, nerve cord and tail region, were each uniquely annotated using a different colour for different segments. Each section of the neuron was checked for the presence of DCVs in it and then annotated. The criteria used to identify a dense core vesicle is mentioned in Table 7.

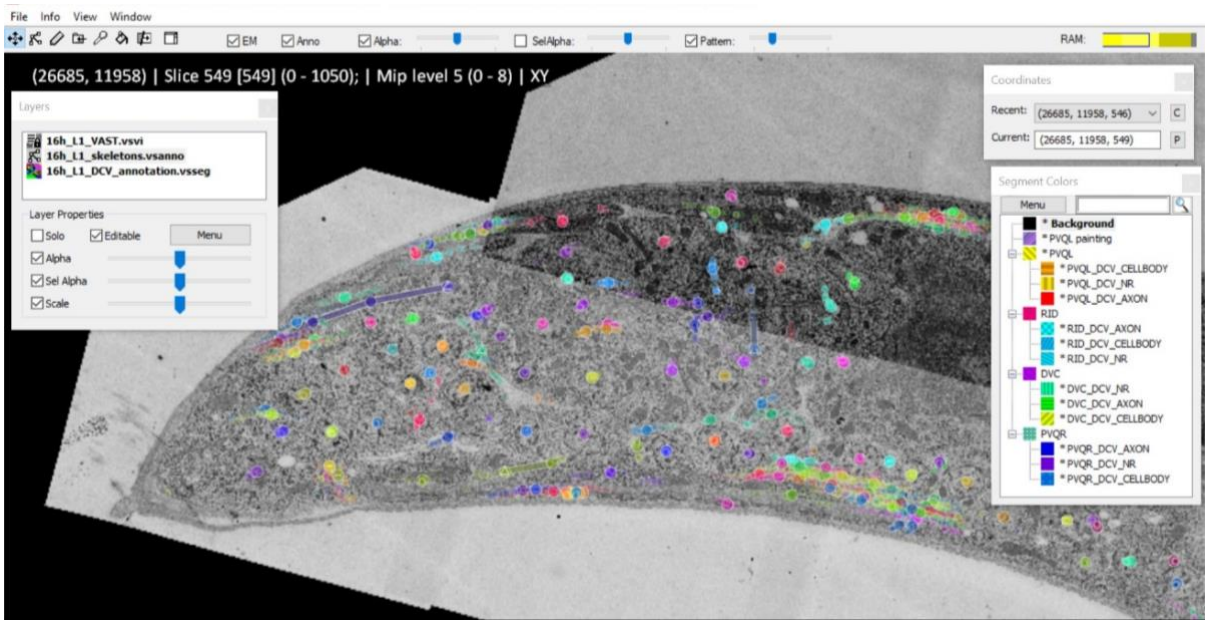

Figure 7. The VAST user interface showing a slide from the EM image stack used in this project. The main window is shown here, featuring multiple movable tool windows, a toolbar for quick access to various editing tools, a toggle to hide all image layers (EM), and sliders to adjust the opacity of the selected segmentation layer (Alpha). Additionally, it includes separate controls for the selected segment or group of segments within the 'Segment Colours' tool window (SelAlpha). The 'Segment Colours' tool window displays a list of all segments used in the chosen segmentation layer, along with their corresponding colours and labels, organized in a tree folder format that illustrates the grouping and relationships between segments and their subparts.

Table 6. The list of neurons that were annotated for DCVs.

PVQL/R (experiment group)
RID (positive control)
DVC (negative control)

Table 7. Criteria listing the parameters used to identify a DCV.

A clear, round outline/shape
Darkly stained (dense core)
Must only be present in one slide, i.e. cannot appear in consecutive slides, as these could be ER.
Darkly stained vesicles near the Golgi apparatus are excluded as they could be ER or other vesicles.

Vesicle must not have any thread-like projections along its outline

5.3. Statistical analysis

For the data obtained from annotation of the EM data set, the annotations for each neuron were classified into three different groups, based on their location – head region, nerve cord region and tail region. This data was used to plot bar graphs using the data analysis & visualization software, Prism (GraphPad).

5.4. Generation of a 3D studio image

A part of the cell body and the ventral nerve cord region of the PVQL neuron, was painted using the annotation tool, VAST. A 3D image was generated by my mentor, Lidia Ripoll-Sánchez, from this segmentation data, using the software Autodesk 3ds max.

6. Generation of IDA-1 knock-in strain

We designed a CRISPR-based IDA-1 knock-in strain for fluorescent labelling of DCVs in a cell-specific manner. The knock-in strain was then generated by a commercial gene editing services company, Suny Biotechnology.

Designing the knock-in strain

To develop CRISPR insert sequence, the sequence viewer application, ApE (A plasmid Editor) was used. The DNA sequence for the only isoform of IDA-1 was obtained from the UCSC genome browser. The sequence for LoxP recognition sites were inserted at the last intron and after the STOP codon of the IDA-1 gene. This was followed by the insertion of the rest of the insert sequence, as mentioned in the results section. The DNA sequence for mNeonGreen, obtained from Shaner et al., 2013.

Results

1. Generation of a PVQ-specific *egl-3* knock out strain using the Cre-LoxP approach

To explore the role of neuropeptidergic signalling specifically in PVQ neurons, we targeted the gene for the EGL-3 protein, a key enzyme in processing neuropeptide precursors. By knocking out the *egl-3* gene, we aimed to disrupt peptidergic signalling in PVQ neurons, allowing us to investigate its impact on behaviours such as locomotion.

A strain was obtained from the Colón-Ramos lab that facilitates endogenous knockout of the *egl-3* gene in a cell-type specific manner (Marquina-Solis et al., 2022). This strain was developed through targeted genome editing using the CRISPR/Cas9 technique, where the *egl-3* gene locus was replaced with a donor template by homology-directed repair. The donor template included two LoxP sites flanking the *egl-3* gene ("floxed egl-3") followed by an mCherry sequence, serving as a reporter for validating the knockout upon expression of Cre recombinase.

Using this strain, we developed a new strain, IBE815, by injecting a plasmid carrying a construct that enables PVQ neuron-specific expression of Cre recombinase. As mentioned in the methods and materials, section 3, this process involved molecular cloning, microinjection, selection of transgenic strains, and subsequent validation of the strain. The expression of Cre recombinase was driven by the promoter for *nlp-17* (CeNGEN), which is specific to the PVQ neuron class. Consequently, the *egl-3* gene was selectively knocked out in PVQ neurons, disrupting peptidergic signalling in these neurons. The successful knockout was indicated by the expression of mCherry, confirming the disruption of *egl-3* in the PVQ neurons.

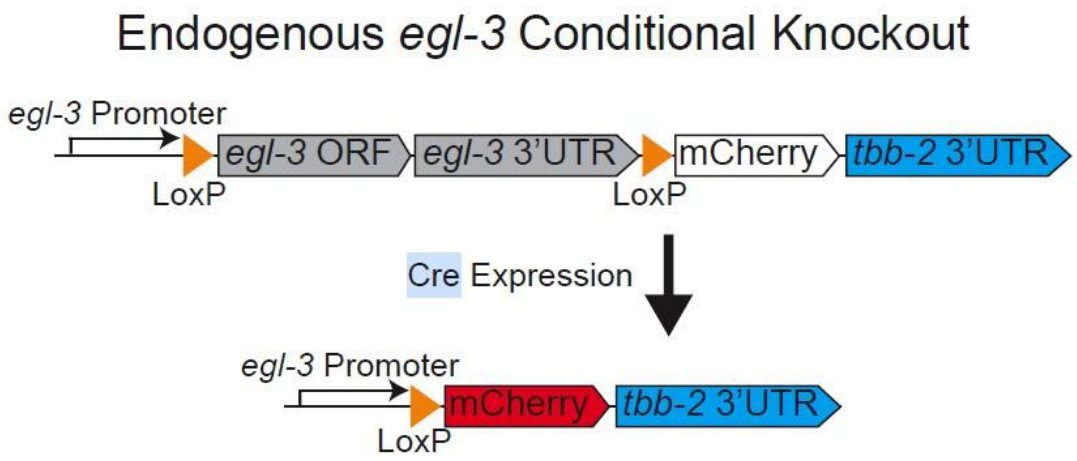

Figure 8. An illustration of the approach for knocking out the endogenous *egl-3* gene in a cell-specific manner. Through targeted genome editing, the *egl-3* gene locus was replaced with a donor template carrying two LoxP sites flanking the *egl-3* gene ("floxed *egl-3*") followed by an mCherry sequence. In the *egl-3*-floxed strain, Cre recombinase is expressed in specific cells to knock out the *egl-3* gene, enabling targeted cells to express mCherry. (Marquina-Solis et al., 2022).

Validating the transgenic knockout

The successful knockout of *egl-3* gene would allow expression of the red fluorescent protein, mCherry. Therefore, to validate the knockout of *egl-3* in our newly generated strain, IBE815, the mutant worms were visualized under confocal microscopy. The red fluorescence from mCherry expression was observed at the expected location of PVQL and PVQR neurons, conforming the successful knockout of the *egl-3* gene.

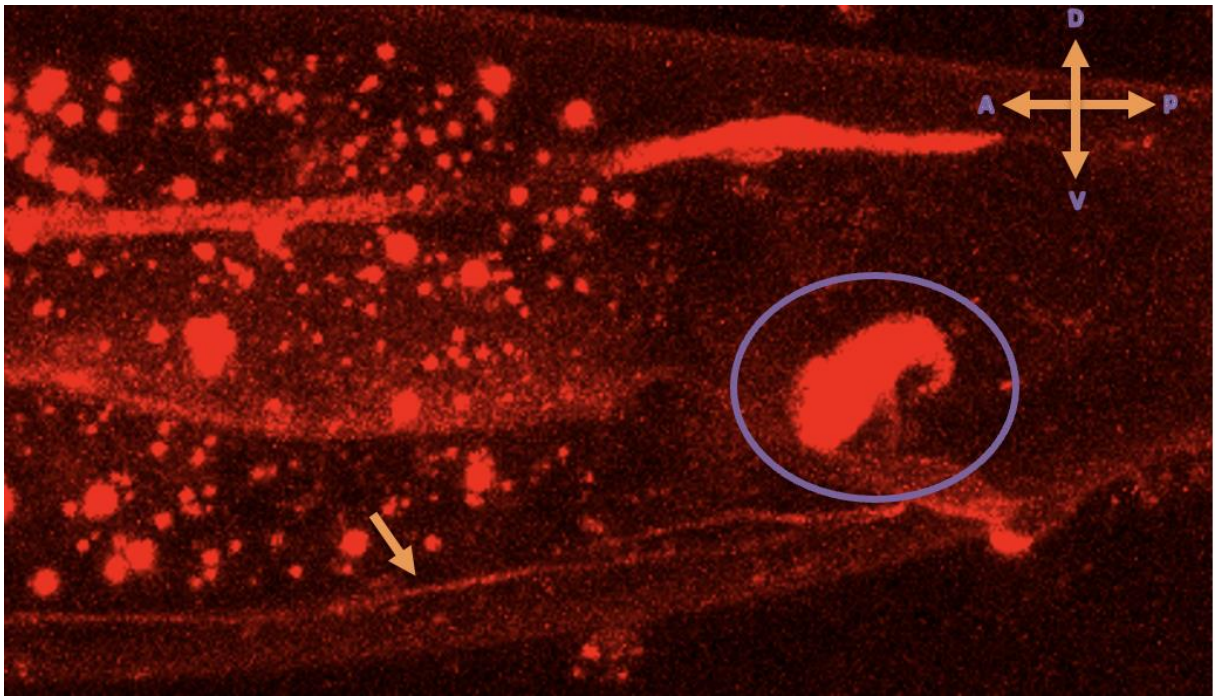

Figure 9. Visualization of fluorescence from mCherrry proteins validates the knockout of *egl-3* gene in PVQ neurons. On visualization of the knockout mutant worms (PVQ-specific *egl-3* knockout) under confocal microscopy, the fluorescence was observed at the expected location of PVQL and PVQR neurons, at the left and right lumbar ganglion respectively, of the tail region. The purple-coloured circle highlights the location of the cell body region, while the orange-coloured arrow indicates the nerve process of PVQ neuron in the ventral nerve cord region.

Following the generation and validation of the IBE815 strain, we conducted locomotion-related behavioral assays to study the impact of disrupted peptidergic

signaling on behaviour. These assays were designed to investigate the role of peptidergic signaling in generating locomotion behavior, providing insights into the functional consequences of *egl-3* gene knockout in PVQ neurons.

2. Disruption of peptidergic signalling in PVQ neurons lowers the rate of forward locomotion

Locomotion-related behavior is a key output of the nervous system's activity. Changes in the nervous system's function typically manifest as abnormalities in locomotion. In the draft neuropeptidergic connectome of *C. elegans* developed by Ripoll-Sánchez et al., it was predicted that PVQ neurons form numerous peptidergic connections with motor neurons of the VB and DB classes. These motor neurons innervate the ventral and dorsal body wall muscles, respectively, establishing neuromuscular junctions in these areas and playing a critical role in forward locomotion and proprioception. Therefore, the disruption of peptidergic signalling in PVQ neurons would in turn disrupt its communication with downstream neurons, such as VB and DB neurons. Since these are motor neurons, we hypothesized that disrupting peptidergic signalling in PVQ neurons would result in a locomotion-related phenotype.

To investigate the functional role of neuropeptidergic signaling in PVQ neurons, knockout mutant worms were analyzed for interesting behavioral phenotypes during spontaneous locomotion. A preliminary behavioral analysis was conducted to quantify the locomotion rate and reversal frequency, parameters that can be easily observed and quantified manually. These measurements were taken during the roaming state of worm locomotion. However, due to time constraints, I was unable to record the locomotion assay for all the controls (N2 wild type and positive control) in this project, which may affect the robustness of the data analysis.

It was observed that the knockout worms showed a decreased rate of body bends/minute relative to the negative control worms, the *egl-3* floxed strain (strain without knocking out of *egl-3*). A nearly 50% reduction in the rate of bends/minute was observed for the knockout worms (p-value = 0.0099) (Figure 10(A)). Additionally, the reversal frequency of the worms was also investigated. It was observed that the number of reversals made per minute did not differ between the knockout mutant worms and the negative control worms. This can be interpreted from the non-significant difference in the mean reversal frequency values between the two strain (p-value = 0.8373). Therefore, it appears that the loss of neuropeptidergic signalling in PVQ neurons affects forward locomotion in worms by decreasing the rate of forward locomotion. These findings suggest that neuropeptidergic signaling in PVQ neurons plays a role in regulating forward locomotion.

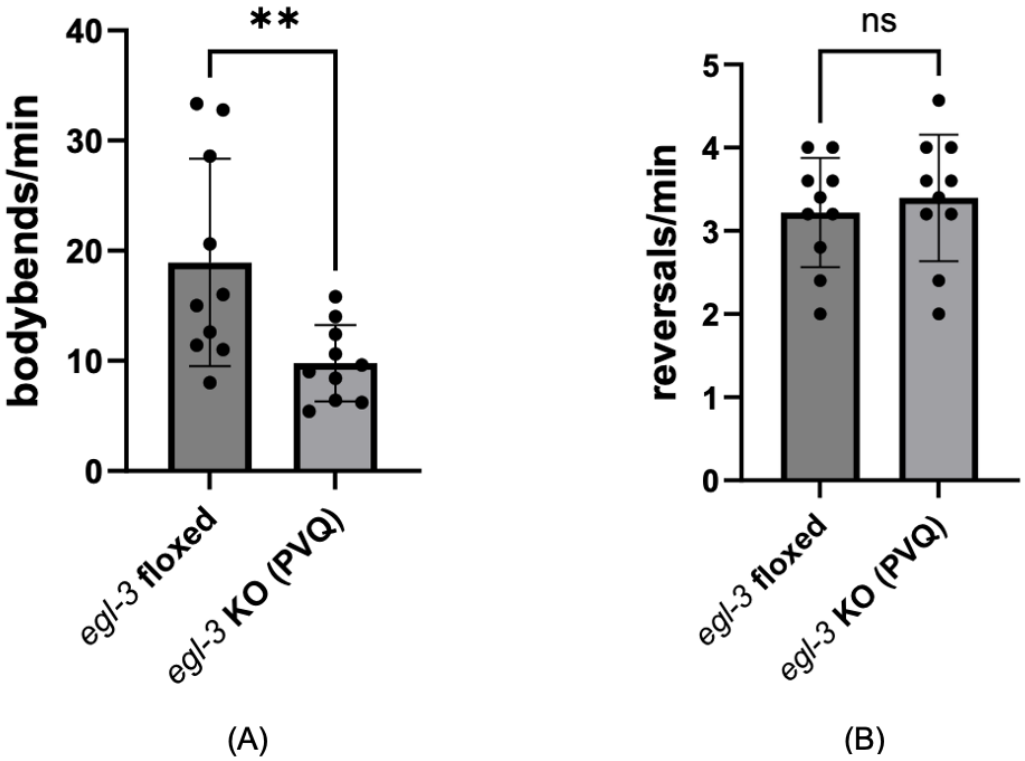

Figure 10. The rate of forward locomotion is lowered in PVQ-specific *egl-3* knockout worms. Spontaneuos locomotion behaviour was analyzed for PVQ-specific egl-3 knockout worms (disrupted peptidergic signalling) and for the *egl-3* floxed worms (no knock out of *egl-3* gene - the negative control). (A) It was observed that the knockout worms exhibited nearly a 50% decrease in the rate of body bends per minute compared to the negative control worms, with a p-value = 0.0099. (B) The reversal frequency of knockout worms did not differ significantly from that of the negative control worms, with a p-value = 0.8373. Therefore, the loss of neuropeptidergic signalling in PVQ neurons affects forward locomotion in worms by decreasing the rate of forward locomotion. N = 10 animals/genotype. P-values ≤ 0.05, 0.01, 0.001 are represented as (*), (**) and (***), respectively. P-value > 0.05 as ns.

Caveats in experimental design

With respect to the experimental design of the locomotion assay, some caveats were observed in the approach used for tracking of worm locomotion. As mentioned previously, due to limitations in time, only the knockout mutant group (IBE815) and the negative control group (DCR6978) were recorded for their locomotion. Ideally, the positive control group (a pan-neuronal *egl-3* knockout strain), a strain that only expresses the PVQ driver construct (*nlp-17p*::Cre) (to ensure that Cre expression does not induce locomotion defects on its own) and the N2 wild-type worms would also be tracked for their locomotion. Additionally, the two different strains used in this experiment were recorded on different days. Since behavioural responses can vary

from day-to-day due to factors such as humidity and temperature of the recording room, dryness of plates, etc, its important for assays with the control and the experimental strains be carried on the same day and on more than one day, ensuring reproducibility and consistency.

3. Distribution characteristics of DCVs in PVQ, RID and DVC class of neurons.

Electron microscopy generates high-resolution images at the nanometer scale, allowing visualization of cellular and subcellular structures with exceptional detail (Subramaniam, 2005). This technique is particularly useful for visualizing dense-core vesicles (DCVs) in neurons, as it provides detailed morphological information and valuable quantitative data, including the number and distribution of DCVs (Witvliet et al., 2021; Hammarlund et al., 2008). Additionally, electron microscopy can reveal structural details such as synaptic connections, membrane structures, and intracellular organelles, which are crucial for understanding neuronal function and organization (Oikonomou, 2017).

In this thesis, we utilized electron microscopy images of the *C. elegans* nervous system during the L1-L2 transition stage (Witvliet et al., 2021). By analysing these high-resolution images, we aimed to gain insights into the morphological characteristics of the distribution of neuropeptide-carrying dense-core vesicles (DCVs) within PVQ neurons. This approach helps investigate the role of extrasynaptic neuropeptidergic signalling in the nervous system of *C. elegans*.

DCVs act as markers for neuropeptidergic signalling because they store and release neuropeptides, which are key extrasynaptic signalling molecules in neurons. By annotating DCVs in EM images, we can map the anatomical distribution of these vesicles within PVQ neurons. This detailed morphological analysis allows us to understand the spatial arrangement of neuropeptide-carrying vesicles and their potential release sites.

To achieve this, the neurons belonging to the classes of PVQL/R, RID, and DVC were traced individually across the slides of the EM images, from the beginning of each neuron to the last slide showing their neuronal process. These slides were annotated for the presence of dense-core vesicles (DCVs). As mentioned in the introduction, PVQ neurons were specifically traced for DCVs due to their position as one of the highest degree hub neurons in the putative neuropeptidergic connectome *of C. elegans* (Ripoll-Sánchez et al., 2023). RID and DVC neurons served as positive and negative controls, respectively.

Like PVQ neurons, RID and DVC neurons have long processes that extend from the cell body across the dorsal and ventral nerve cords, respectively (White et al., 1986b). Additionally, both RID and PVQ neurons are classified as modulatory neurons, which do not express classical neurotransmitters or monoamines (Wang et al., 2024b; Witvliet et al., 2021; Lim et al., 2016). This shared characteristic is why we chose RID as the positive control.

In contrast, DVC neurons have a relatively low number of neuropeptidergic connections, making them suitable as a negative control in this study (Ripoll-Sánchez et al., 2023). By examining the presence and distribution of DCVs in these neurons, we can better understand the mechanisms of neuropeptide release and their impact on neuronal communication and behaviour, such as locomotion.

The PVQL and PVQR neuron somas are located in the left and right lumbar ganglia, respectively, in the tail region, where PVQ neurons are born. The total number of dense-core vesicles (DCVs) observed was 443 in PVQL and 179 in PVQR (Figure 5). In the cell body region of these neurons, very few DCVs were detected. Specifically, PVQL had 9 DCVs, which accounts for 2% of its total DCVs, while PVQR had 3 DCVs, making up 1.67% of its total DCVs. In comparision, the neuronal processes in the nerve ring region had the highest abundance of DCVs, with PVQL containing 77.2% of its total DCVs and PVQR containing 83.79% of its total DCVs. A significant number of DCVs were also observed in the ventral nerve cord region, with PVQL containing 20.67% and PVQR containing 14.52% of their total DCVs. Additionally, it was noted that the PVQL neuron had more than twice the number of DCVs compared to the PVQR neuron, with PVQL having 443 DCVs and PVQR having 179 DCVs (Table 8).

In addition to this, during the tracing and annotation of DCVs in PVQ neurons, I observed that DCVs often tend to be clustered together in the ventral nerve cord region. (Figure 11(A and C)). Additionally, these clusters of DCVs were frequently found in specific locations: around synapses, along the edges of a neuronal process, and in proximity to mitochondria.

In comparision, RID neuron, with its soma situated in the nerve ring region, exhibited a distribution pattern of DCVs different from that of PVQL and PVQR neurons, representing different DCV localization preferences (Figure 5). RID shows a relatively smaller total DCV count of 52. In RID neuron, the neuronal processes within the dorsal nerve cord region appears to be the primary storage region for DCVs, with approximately 80.77% of the total DCVs concentrated in this region. This region has a higher abundance of DCVs compared to the nerve ring region, which contains approximately 9.62% of the total DCVs. Similarly, the cell body region of RID contains a comparable proportion of DCVs, also around 9.62% of the total DCVs (Table 8). This distribution pattern may be representative of the functional specialization of RID neuron

within the neural circuitry, where the dorsal nerve cord region acts as a DCV storage and release point, distinct from the distribution observed in PVQ neurons.

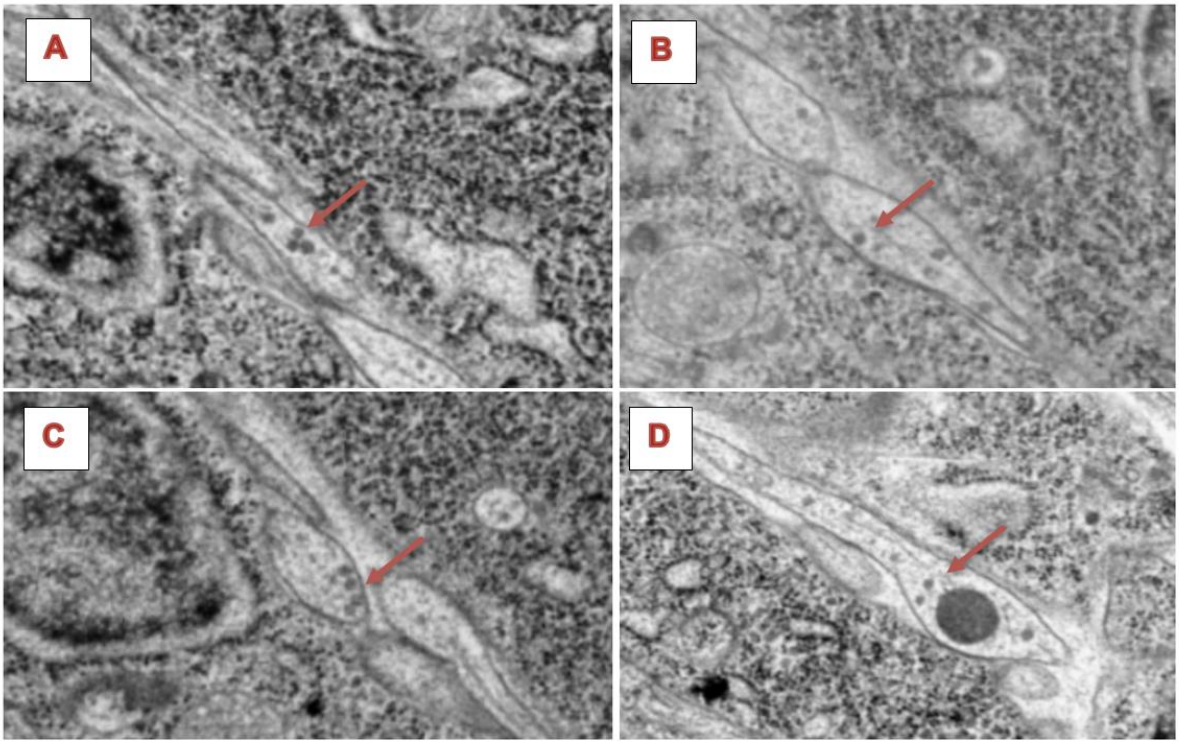

Figure 11. EM images of PVQL neuron representing the common clustering patterns of DCVs within the nerve cord region. When tracing the EM images of PVQ neurons, it was observed that (A) DCVs exhibit a propensity to form clusters, particularly in distinct regions: around synaptic junctions, (B and C) along the periphery of neuronal processes, and (D) in close proximity to mitochondria. These observations suggest potential functional associations between DCV clustering patterns and synaptic activity or energy metabolism within PVQ neurons.

Similar to PVQ neurons, DVC neuron demonstrate a greater accumulation of DCVs in the nerve ring region, where approximately 77.97% of the total DCVs are localized. The high prevalence of DCVs in the nerve ring mirrors the distribution pattern observed in PVQ neurons. Additionally, DVC neurons have significant number of DCVs in the dorsal nerve cord region, approximately 15.25% of the total DCVs. Like PVQ neurons, DVC display a relatively limited concentration of DCVs in the cell body region, constituting of around 1.69% of the total DCVs (Table 8). With a total of 118 DCVs, DVC neuron has a greater DCV count than in RID neuron, showcasing an intermediate position in terms of overall DCV quantity among the studied neurons.

Table 8: Distribution of Dense-Core Vesicles (DCVs) in PVQL, PVQR, RID, and DVC Neurons

Neuron	Total DCVs	DCVs in Cell Body (%)	DCVs in Nerve Ring (%)	DCVs in Ventral/Dorsal Nerve Cord (%)
PVQL	443	9 (2.0%)	342 (77.2%)	92 (20.7%)
PVQR	179	3 (1.7%)	150 (83.8%)	26 (14.5%)
RID	52	5 (9.6%)	5 (9.6%)	42 (80.8%)
DVC	118	2 (1.7%)	92 (78.0%)	18 (15.3%)

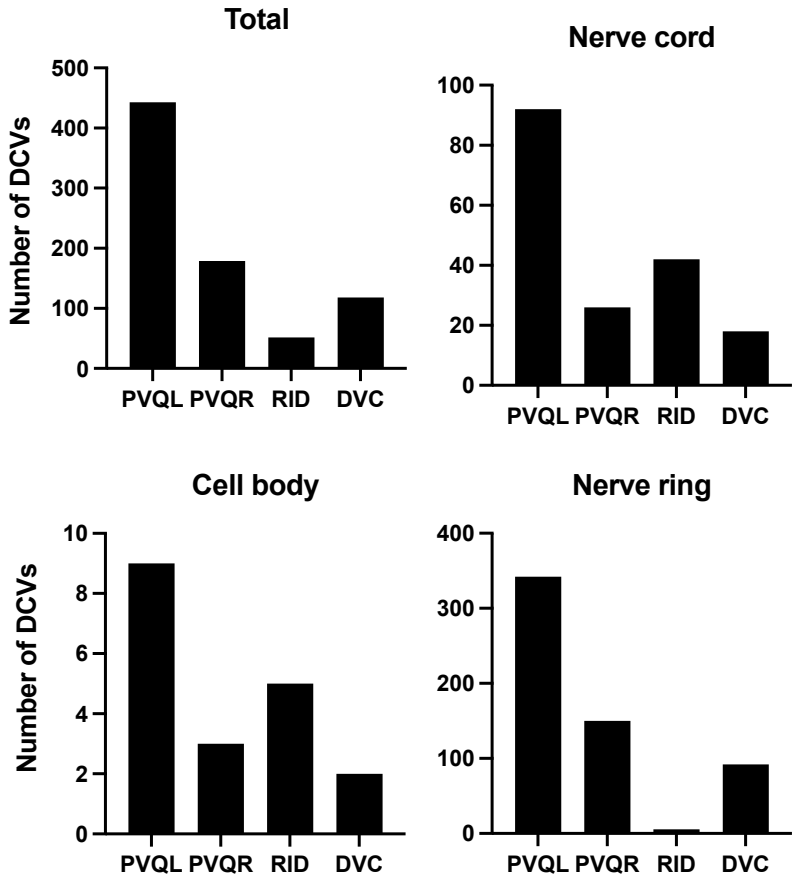

Figure 12: Graphical representation illustrating the distribution of dense-core vesicles (DCVs) in experimental and control group neurons. PVQL/R, RID, and

DVC neurons were traced and annotated for DCVs. Notably, PVQ neurons have few DCVs in their cell bodies, with the nerve ring region being the most enriched in DCVs for both PVQL and PVQR. Furthermore, a significant number of DCVs are observed in the ventral nerve cord region of PVQ neurons. DVC neuron demonstrates a DCV distribution pattern similar to that of PVQ neurons. In contrast, RID neurons display a higher abundance of DCVs in the dorsal nerve cord region compared to the nerve ring and cell body regions. Additionally, PVQL neurons exhibit more than double the number of DCVs compared to PVQR neurons. (Experimental group = PVQL/R, negative control = DVC, positive control = RID).

To investigate the potential link between the reduced presence of dense-core vesicles (DCVs) in the nerve ring and neuropeptide secretion levels, my mentor, Lidia Ripoll-Sánchez, conducted an analysis. This analysis aimed to map the neuropeptide-GPCR pairings along RID's length to identify the putative peptidergic connections RID was forming with other neurons (see Figure 13). It was found that neurons in the nerve ring region had fewer GPCR receptors for RID neuropeptides compared to those in the dorsal nerve cord, suggesting a lower demand for neuropeptide expression in RID and thus fewer DCVs in this region. Additionally, neurons with processes in the ventral nerve cord (VNC) were observed to have GPCR receptors for RID neuropeptides, indicating a greater need for neuropeptide expression in this area. This could explain the higher accumulation of DCVs in the dorsal nerve cord region of the RID neuron.

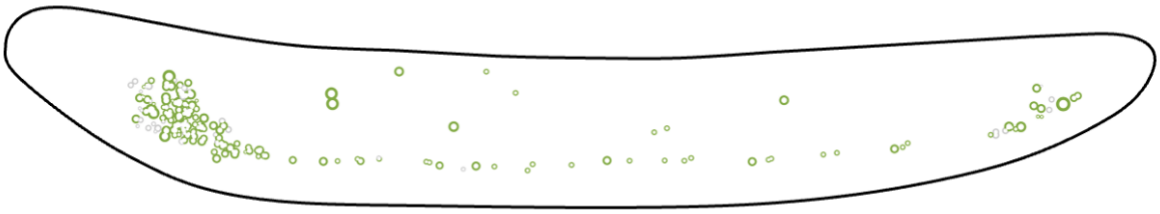

Figure 13: Location of peptidergic connections between RID and other neurons in *C. elegans*. The spheres in the illustration depict the cell bodies of neurons, with their size reflecting the quantity of neuropeptide-GPCR pairs present in each neuron. Green-coloured neurons indicate those that express a receptor for RID, whereas neurons marked with a white dot express a neuropeptide. Neurons shown in grey do not express the receptor. Consequently, RID seems to establish numerous connections with various neurons throughout the worm's body.

In the EM image slides, a section of the PVQL neuron was painted using the VAST segmentation tool to enable 3D visualization of this region and the DCVs within it. The rendering of a 3D image was performed by my daily mentor, Lidia Ripoll-Sánchez. As mentioned earlier, the soma of PVQ neurons, which include PVQL and PVQR, are anatomically situated in the left and right lumbar ganglia in the tail region, respectively, and extend their neuronal processes anteriorly towards the nerve ring. The visualization included a portion of the cell body and the VNC region.

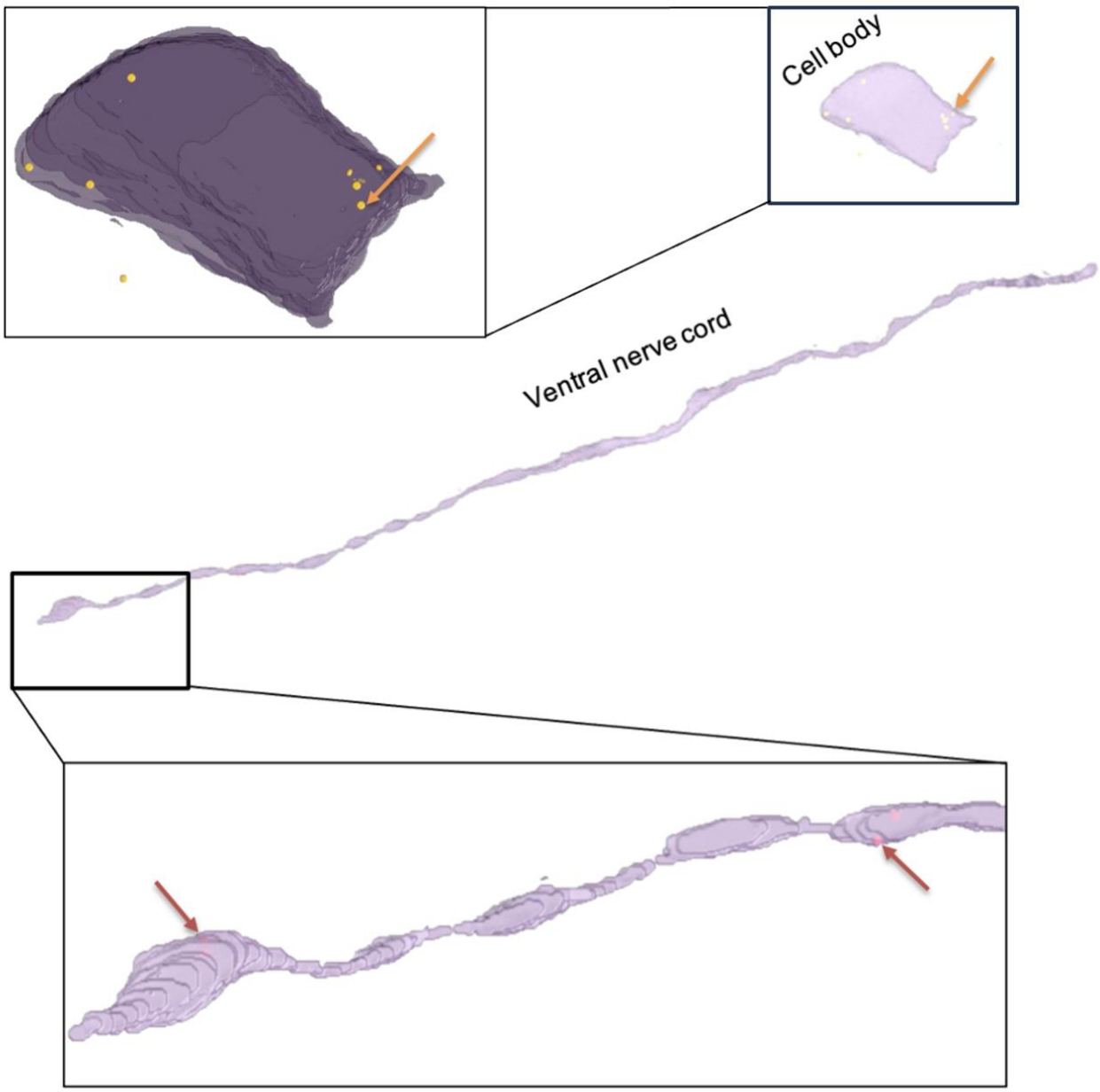

Figure 14. A 3D visualization of a part of the cell body and ventral nerve cord (VNC) region in PVQL neuron with highlighted DCVs. PVQL neurons, located in the left lumbar ganglia in the tail region, extend their processes anteriorly towards the nerve ring. The DCVs observed in the cell body region were concentrated in the region extending into the neuronal process. The DCVs in the VNC neuronal processes were clustered together in neuronal boutons. DCVs in the cell body are denoted by yellow circles, while those in the VNC by pink circles.

In the cell body region, several of the DCVs are present localized to the region extending into the neuronal process of PVQL. This suggests transportation of DCVs from the cell body towards the neuronal processes in the VNC. This indicates a

dynamic process of DCV trafficking from the cell body to the neuronal process of the neuron.

Although it is difficult to locate the DCVs in the VNC region due to poor resolution caused by the zoomed-out image, it is evident that the DCVs in this area also frequently form clusters and are present in neuronal boutons. This visualization provides insights into the spatial distribution of DCVs within different regions of the PVQL neuron.

4. A CRISPR knock-in strain was designed for fluorescence-based visualization of DCVs

Visualizing endogenously expressed dense-core vesicles (DCVs) in a cell-specific manner enables the study of their movement, distribution, and density within specific neurons in real-time. Understanding these aspects of DCV dynamics allows us to investigate the anatomical aspects of peptidergic signalling in PVQ neurons.

To achieve this, we designed a strain to facilitate DCV visualization by fluorescently labelling the DCV marker protein IDA-1. IDA-1 is a transmembrane receptor tyrosine phosphatase-like protein found on DCVs, potentially playing a role in the regulation of DCV trafficking and secretion (Zahn et al., 2004b). For this study, IDA-1 was tagged with a bright green fluorescent protein, mNeonGreen, at its cytosol-facing C-terminal (Hostettler et al., 2017; Zahn et al., 2004a), allowing for real-time visualization of DCVs within neurons.

The donor template design for the CRISPR-based knock-in was developed to maintain endogenous expression levels of IDA-1 while incorporating the fluorescent tag. This design is illustrated in the figure below (Figure 15). In this design, a Cre-LoxP approach is used to label IDA-1. LoxP recognition sites flank parts of the last intron, the last exon, and the STOP codon of the IDA-1 gene. Following this sequence is the gene for mNeonGreen, preceding the STOP codon (Figure 15(B)). Expression of Cre recombinase in specific neurons results in the excision of the LoxP-flanked sequence, thereby allowing the expression of IDA-1 fused with the fluorescent tag on DCV surfaces (Figure 15(C)).

This knock-in strain, named PHX9058, was developed in collaboration with Suny Biotechnology, a commercial gene editing service provider. For cell-specific DCV labelling, a plasmid containing Cre recombinase under the control of a cell-specific promoter can be introduced.

In cases where a strong, specific promoter is not available for the neuron of interest, a dual recombinase approach can be employed. This involves using two plasmids carrying Flp and Cre recombinase genes, each under the control of promoters with

overlapping expression patterns, thus implementing an "AND" gate strategy for cell-specific gene expression (Ge et al., 2020).

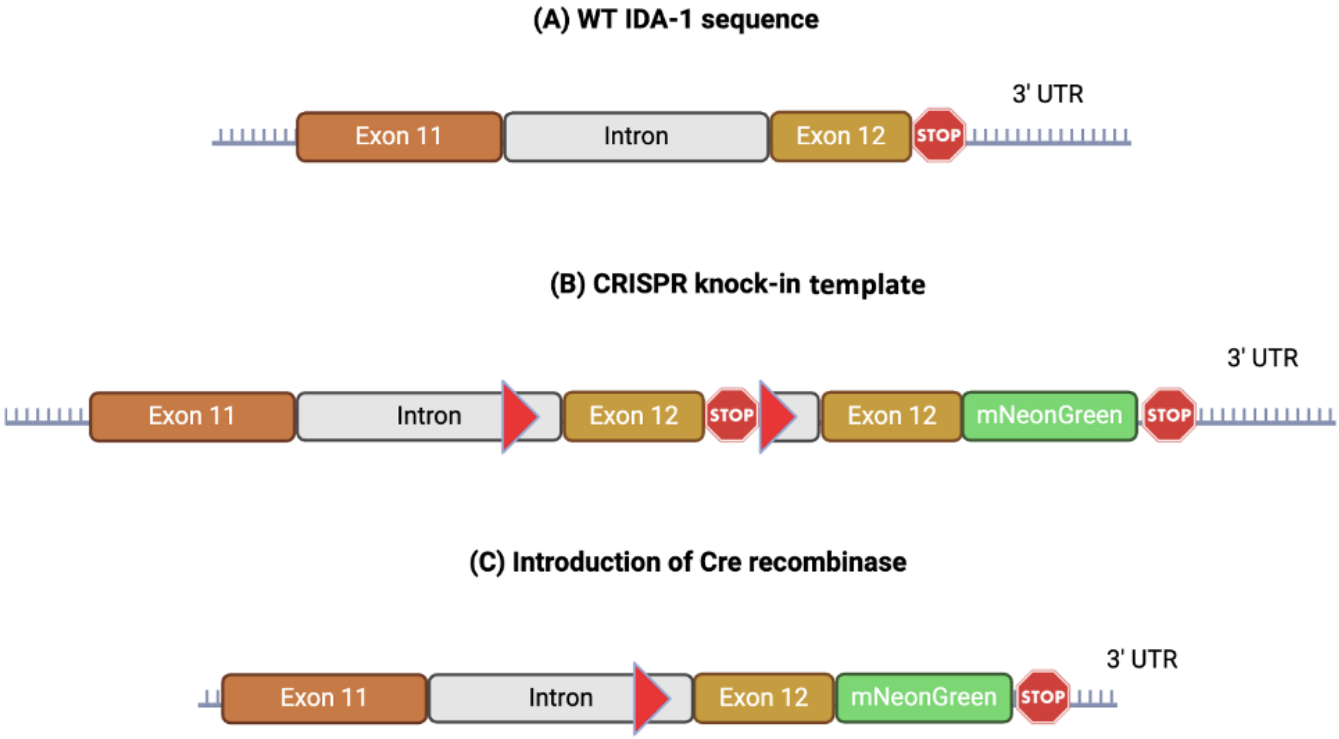

Figure 15: The design of a knock-in strain (PHX9058) for endogenous and cell-specific labelling of DCVs. (A) The wild-type *C. elegans* genome has a single copy of the IDA-1 gene on chromosome III, consisting of a series of 12 exons, encoding a type-1 transmembrane protein. (B) The CRISPR knock-in strain has LoxP recognition sites flanking a part of the last intron, the last exon, and the STOP codon. (C) Expression of Cre recombinase cleaves out the floxed region, allowing expression of a fusion protein of IDA-1 and mNeonGreen.

To validate the functioning of the obtained strain, a plasmid carrying Cre recombinase under a pan-neuronal promoter was expressed (Figure 16). This was carried out by my daily mentor, Jun Meng. A bright green fluorescence was observed in the expected regions—the nerve ring region in the head, the tail ganglia at the posterior end, and along the dorsal and ventral nerve cord regions—confirming the effective tagging of IDA-1 and its expression in the neurons.

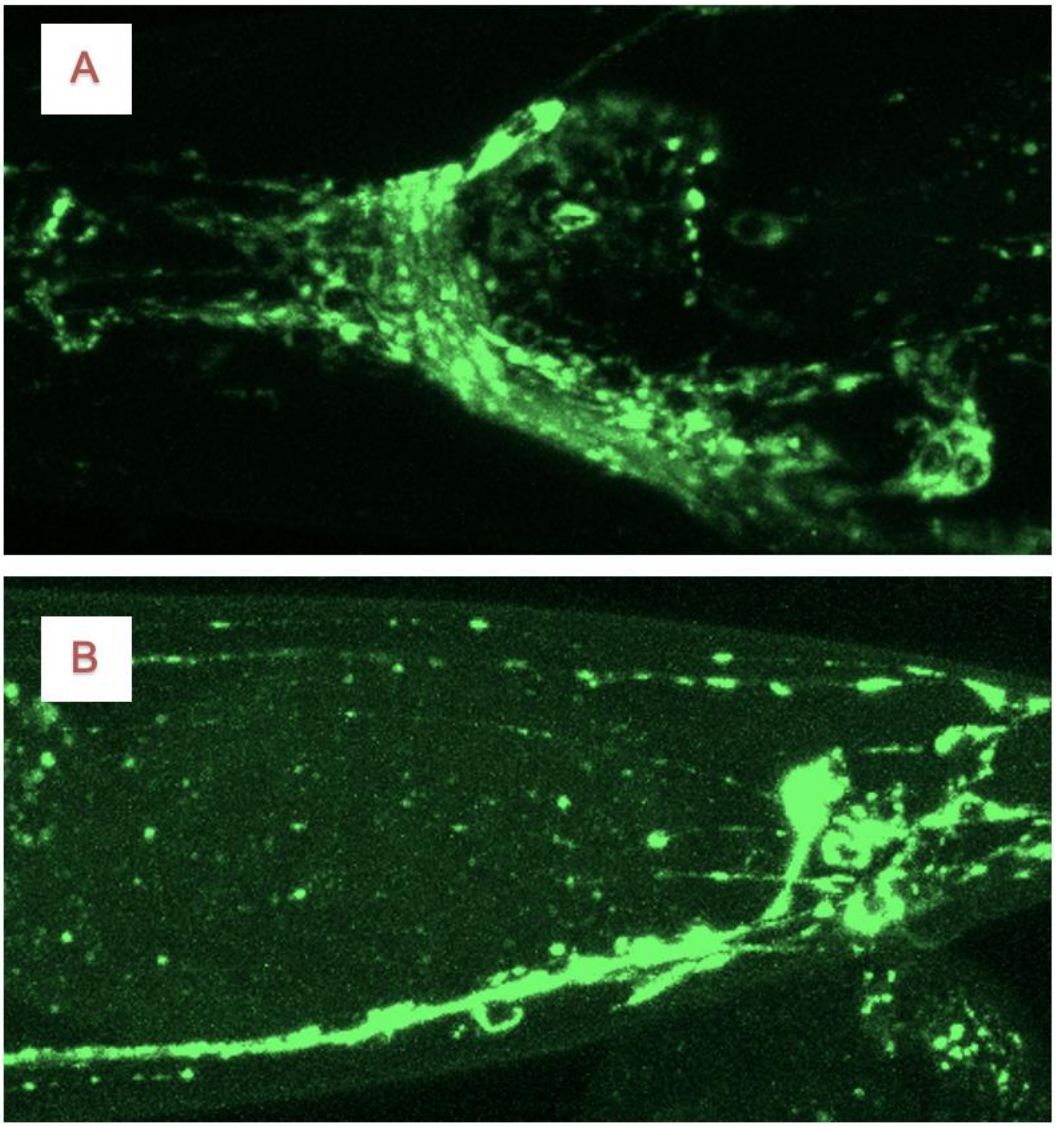

Figure 16: Visualization of fluorescently tagged DCVs in all the neurons of *C. elegans.* Expression of Cre recombinase under a pan-neuronal promoter in strain PHX9058 resulted in bright green fluorescence (A) in the nerve ring, (B) in the tail ganglia, and the dorsal and ventral nerve cords. This confirms effective tagging of IDA-1 with mNeonGreen and successful visualization of dense-core vesicles (DCVs) in neurons.

Discussion

1. Neuropeptidergic signalling in PVQ neurons may play a role in forward locomotion.

Locomotion is one of the major behavioural outputs of the nervous system. Important signalling molecules, such as neuropeptides, modulate a diverse range of behaviours in *C. elegans,* including locomotion. Therefore, in this study, we expected that the disruption of neuropeptidergic signalling in PVQ neurons would ultimately present a behavioural phenotype related to locomotion (Chang et al., 2015b; Choi et al., 2015). In this project, we explored the role of extrasynaptic signalling in PVQ neurons through a spontaneous locomotion assay of *egl-3* knockout worms.

It was observed that the knockout mutant worms showed a 50% reduction in body bends/minute compared to the negative control worms, the *egl-3* floxed strain. However, the reversal frequency did not differ between the knockout mutant worms and the negative control worms. This indicates that the loss of neuropeptidergic signalling in PVQ neurons affects forward locomotion in *C. elegans*. This is in consensus with a previous study by Ripoll-Sánchez et al., that developed a draft connectome for neuropeptidergic signalling in *C. elegans*.

As mentioned previously, PVQ neurons are predicted to form many connections with neurons belonging to the classes URX, PQR, BAG, BDU, VB and DB. The neuron classes VB and DB are motor neurons that innervate the ventral and dorsal body wall muscles, which play an important role in forward locomotion and proprioception. In fact, VB and DB class of neurons are involved in the propagation of body bending signals during locomotion (Wen et al., 2012). They are activated by ventral and dorsal bending of an anterior body region, which is followed by the propagation of the bending signal by these neurons in the posterior direction (Wen et al., 2012). Therefore, we hypothesize that disrupting neuropeptidergic signalling in PVQ neurons interferes with propagation of bending signals by VB and DB neurons, which produces the behavioural phenotype of reduced body bends during forward locomotion.

Previous studies have indicated that PVQ neurons are involved in the guidance of axons during the development of VNC in the embryo (Garriga et al., 1993). PVQ class of neurons were also found to be involved in a head-tail-head temperature acclimation circuit. This neural circuit regulated gut fat storage and is comprised of ASJ head thermosensory neurons, PVQ tail interneurons, and RMG head interneurons (Motomura et al., 2022). Finally, in another study, it was found that during sexual behaviour in *C. elegans*, PVQ neurons are targeted by sex-specific neurons (HSN in hermaphrodites and CEM, MCM and EF in males). This indicates that PVQ neurons may be involved in controlling locomotion and integrating sexual and sensory pathways during sexual behaviour in both the sexes.

Our findings indicate that neuropeptidergic signalling in PVQ neurons is essential for forward locomotion. PVQ neurons were found to be involved in regulating the frequency of body bends during spontaneous locomotion in *C. elegans*, likely through their influence on the propagation of bending signals by VB and DB motor neurons.

However, as discussed in the results section, this interpretation is based on preliminary behavioural analysis. To obtain objective and quantitative data, followed by thorough analysis, the locomotion assays need to be redone. The redesigned experiment should include the following changes:

1. Record behaviours for all control groups: negative control (*egl-3* floxed strain), positive control (pan-neuronal *egl-3* knockout strain), a strain that only expresses the PVQ driver construct and wild-type control.
2. Conduct behavioural recordings for all strains, both experimental and control groups, on the same day and across multiple days as biological replicates.

Additionally, it would be valuable to investigate how a reduction in body bend frequency impacts forward locomotion speed and to test for other locomotion-related phenotypes. Moreover, since PVQ neurons are believed to form strong peptidergic connections with neurons involved in oxygen sensing circuits, exploring related behavioural phenotypes would also be interesting.

2. PVQ neurons show the anatomical characteristics of a peptidergic neuron.

Electron microscopy produces high-resolution images that enable the examination of a neuron's ultrastructural details. In this research, the neuron classes PVQ, RID, and DVC were annotated for dense core vesicles (DCVs) within an EM dataset obtained from worms in the L1-L2 transition stage (Witvliet et al., 2021; Mulcahy et al., 2018).

It was observed that DCVs had different distribution patterns across these neuron classes. In PVQ neurons, DCVs were plentiful in the nerve ring region and the ventral nerve cord, with some present in the cell body area. This aligns with Ripoll-Sánchez et al.'s findings, which showed that PVQ neurons form a dense network of connections with other neurons in the short-range network of the nerve ring region. A high number of connections in the putative neuropeptidergic connectome suggests a greater need for neuropeptidergic signalling in the area, therefore requiring the accumulation of DCVs there. The DVC neuron class displayed a similar DCV distribution pattern to PVQ neurons but had fewer overall DCVs, possibly due to forming fewer putative peptidergic connections compared to PVQ neurons (Ripoll-Sánchez et al., 2023).

In addition to this, during the tracing and annotation of DCVs in PVQ neurons, I observed that DCVs can often form clusters, which indicates a potential for localized release of neuropeptides. In the nerve cord region, these clusters of DCVs were frequently found in specific locations: around synapses; along the edges of a neuronal

process; and in proximity to mitochondria, which could indicate a relationship with the energy demands of neuropeptide release. Furthermore, the clustering of DCVs might reflect a mechanism for enhancing the efficiency of neuropeptide release, to ensure a sufficient concentration of neuropeptides are released in the region.

Unlike PVQ neurons, RID neurons were found to have more DCVs in the dorsal nerve cord region compared to the nerve ring region. This distribution might be explained by a higher number of connections in the nerve cord area compared to that in the nerve ring region. To investigate this, an analysis was conducted to map out the connections along RID's length and to indicate whether RID sent or received these connections. It was observed that neurons in the nerve ring region had fewer GPCR receptors for RID neuropeptides than in the dorsal nerve cord. However, there were still enough neurons in the nerve ring with GPCR receptors to not justify the low number of DCVs in RID's nerve ring region. Alternatively, the RID neuronal process in the DNC may have more DCV as there are neurons with processes in the VNC that have GPCR receptors for RID neuropeptides. This increased distance for neuropeptide diffusion (form DNC to VNC) necessitates a higher volume of neuropeptide expression and release, which would require DCVs accumulation in the DNC of RID.

Interestingly, despite being a peptidergic neuron, RID had fewer DCVs compared to PVQ neurons and DVC neuron. This might be due to the dynamic nature of neuropeptide expression and secretion. Consequently, at the time the EM data was collected, RID may not have been actively communicating with other neurons in the region, resulting in the observed low number of DCVs in this data set. Similarly, the greater abundance of DCVs in PVQL neurons compared to PVQR neurons could be due to the higher activity level of PVQL at the time the data was collected. For instance, movement in a specific body region might have necessitated increased activity in the PVQL neuron.

Neurons release neuropeptides through the regulated exocytosis of dense-core vesicles (DCVs). According to Hoover et al., motor neurons in *C. elegans* mainly transport their DCVs to the axons, resulting in few DCVs remaining in the cell bodies. Consistent with this, our study found that the three neuron classes — PVQ, RID, and DVC — do not utilize their cell bodies to store a significant number of DCVs for secretion.

In a study on the olfactory projection neurons (PNs) of *Drosophila melanogaster*, researchers found that presynaptic active zones contained dense-core vesicles (DCVs) and mitochondria (Yang et al., 2021). Similarly, our study observed that DCVs often appeared around synapses, along the membrane of the neuronal boutons, and near mitochondria. Zhao et al. demonstrated that axonal mitochondria are crucial for neuropeptide secretion in *C. elegans*, requiring oxidative phosphorylation for this process. Thus, DCVs may cluster near mitochondria because the mitochondria provide the energy necessary for DCV secretion. A similar observation was made in *C. elegans*

by Witvliet et al., noting that presynaptic swellings were characterized by DCVs, mitochondria, and cadherin-like junctions between pre- and postsynaptic partner cells.

The 3D visualization of the PVQL neuron and the distribution patterns of DCVs offer significant insights into the spatial organization of DCV in different neuronal regions. Future research should focus on expanding our understanding of DCV dynamics.

Firstly, it is essential to collect data on the distribution of synapses and presynaptic active zones along the full length of the neurons. Identifying whether synapses are present or absent in particular regions could indicate areas specialized for synaptic input. Additionally, this information will be valuable for investigating the mechanisms underlying DCV release in this region.

Additionally, obtaining quantitative data on the distribution of DCVs near synapses, mitochondria, and along the membrane would provide valuable insights into the relationship between DCV localization and neuronal function.

3. Visualization of dense-core vesicles in neurons using fluorescently tagged IDA-1 in *C. elegans*

In this study, we have developed a novel approach for visualizing DCVs within specific neurons in real-time, employing fluorescent labelling of the DCV marker protein IDA-1. By strategically tagging IDA-1 with the bright fluorescent protein mNeonGreen, we have enabled the visualization of DCVs in neurons, facilitating the study of their movement, distribution, and density.

The use of a Cre-LoxP approach allowed for cell-specific expression of the tagged IDA-1 protein at endogenous levels.

Visualizing DCVs in worms at various stages of their life cycle can provide insights into how they are distributed within neurons during different developmental phases, allowing us to overcome limitations of data obtained from tracing EM images. While EM images capture DCV distribution in a particular developmental stage, with the IDA-1 strain, the dynamic nature of peptidergic signalling through DCVs can be captured across different developmental stages. This approach enables investigation of changes in DCV distribution and dynamics throughout development, shedding light on the mechanisms underlying peptidergic signalling modulation during different developmental stages.

The expression of Cre recombinase under a pan-neuronal promoter was used to confirm the functionality of our approach. The observed bright green fluorescence in expected neuronal regions demonstrates successful tagging of IDA-1 and its expression within neurons, validating our strategy for visualizing DCVs in neuronal tissue. This approach is similar to previous methods such as that employed by Lim et al., where DCVs were visualized by exogenous expression of an IDA-1::mCherry

fusion protein in the neuronal class, RID. In that study, DCVs were observed to periodically accumulate at specific locations along the RID neuronal process, forming a pearling pattern.

In the future, the IDA1 knock-in strain for visualizing dense-core vesicles (DCVs) could be used to explore several exciting research questions in the field of neurobiology.

Using this approach, specific subsets of neurons could be targeted using cell-specific promoters or by using dual recombinase strategies. This would enable us to study the variation of DCV dynamics across different neuronal populations.

Secondly, time-lapse studies of this strain would allow the observation of DCV dynamics throughout the life cycle of worms. This could uncover novel insights into the regulation of peptidergic signalling during worm development. By tracking changes in DCV distribution and density at different developmental stages, allowing us to study changes in peptidergic signalling during development-related changes in *C. elegans*.

Finally, by visualizing and observing the movement of DCVs in real-time, we can gain deeper insights into DCV trafficking and release in neurons.

Conclusions

This thesis has provided novel insights into the role of neuropeptidergic signalling in PVQ neurons and their impact on locomotion in *C. elegans*. Through this research project, our findings have enhanced our understanding of neuropeptidergic connectomics.

Our findings indicate that neuropeptidergic signalling in PVQ neurons plays a role in regulating forward locomotion. Using a spontaneous locomotion assay with *egl-3* knockout worms, we observed a 50% reduction in body bends per minute compared to the control group. This reduction highlights the significant role of PVQ neurons in modulating forward locomotion, likely through their influence on the propagation of bending signals by VB and DB motor neurons.

Furthermore, anatomical studies using electron microscopy revealed that PVQ neurons display the characteristics of peptidergic neurons, with a strong presence of dense core vesicles (DCVs) in the nerve ring region and the ventral nerve cord. The clustering of DCVs around synapses and mitochondria suggests possible mechanisms for efficient neuropeptide release.

The design of a novel method for visualizing DCVs in neurons through the fluorescent tagging of marker protein IDA-1 will allow us to study the dynamics of DCVs in real time, in different neuronal populations and across worm developmental stages.

In conclusion, this thesis advances our knowledge of the functional and anatomical aspects of neuropeptidergic signalling in PVQ neurons and their role in locomotion. These findings lay the groundwork for future research to understand the broader implications of neuropeptidergic modulation in neural function and behaviour.

References

Agnati, L. F., Fuxe, K., Zoli, M., Ozini, I., Toffano, G., & Ferraguti, F. (1986). A correlation analysis of the regional distribution of central enkephalin and β-endorphin immunoreactive terminals and of opiate receptors in adult and old male rats. Evidence for the existence of two main types of communication in the central nervous system: the volume transmission and the wiring transmission. *Acta Physiologica Scandinavica*, *128*(2), 201–207. https://doi.org/10.1111/J.1748-1716.1986.TB07967.X

Agnati, L. F., Zoli, M., Pich, E. M., Benfenati, F., Zini, I., Fuxe, K., & Goldstein, M. (1986). Aspects on the information handling by the central nervous system: focus on cotransmission in the aged rat brain. *Progress in Brain Research*, *68*(C), 291–301. https://doi.org/10.1016/S0079-6123(08)60245-9

AlHarbi, S., & Frøkjær-Jensen, C. (2023). Characterizing a standardized BioPart for PVQ-specific expression in *C. elegans*. *MicroPublication Biology*, *2023*. https://doi.org/10.17912/MICROPUB.BIOLOGY.000870

Beets, I., Zels, S., Vandewyer, E., Demeulemeester, J., Caers, J., Baytemur, E., Courtney, A., Golinelli, L., Hasakioğulları, İ., Schafer, W. R., Vértes, P. E., Mirabeau, O., & Schoofs, L. (2023). System-wide mapping of peptide-GPCR interactions in *C. elegans*. *Cell Reports*, *42*(9), 113058. https://doi.org/10.1016/J.CELREP.2023.113058

Bennett, M. V. L., & Zukin, R. S. (2004). Electrical Coupling and Neuronal Synchronization in the Mammalian Brain. *Neuron*, *41*(4), 495–511. https://doi.org/10.1016/S0896-6273(04)00043-1

Bentley, B., Branicky, R., Barnes, C. L., Chew, Y. L., Yemini, E., Bullmore, E. T., Vértes, P. E., & Schafer, W. R. (2016). The Multilayer Connectome of *Caenorhabditis elegans*. *PLoS Computational Biology*, *12*(12). https://doi.org/10.1371/journal.pcbi.1005283

Berger, D. R., Seung, H. S., & Lichtman, J. W. (2018). VAST (Volume Annotation and Segmentation Tool): Efficient manual and semi-automatic labeling of large 3D image stacks. *Frontiers in Neural Circuits*, *12*, 406276. https://doi.org/10.3389/FNCIR.2018.00088/BIBTEX

Bernardo Sabatini, & Morgan Sheng. (2012). *The Synapse* . Barnes & Noble.

Beverly, M., Anbil, S., & Sengupta, P. (2011). Degeneracy and Neuromodulation among Thermosensory Neurons Contribute to Robust Thermosensory Behaviors in *Caenorhabditis elegans*. *Journal of Neuroscience*, *31*(32), 11718–11727. https://doi.org/10.1523/JNEUROSCI.1098-11.2011

Beyer, J., Troidl, J., Boorboor, S., Hadwiger, M., Kaufman, A., & Pfister, H. (2022). A Survey of Visualization and Analysis in High-Resolution Connectomics. *Computer Graphics Forum*, *41*(3), 573–607. https://doi.org/10.1111/CGF.14574

Brenner, S. (1974). The genetics of *Caenorhabditis elegans*. *Genetics*, *77*(1), 71–94. https://doi.org/10.1093/GENETICS/77.1.71

Briggman, K. L., & Bock, D. D. (2012). Volume electron microscopy for neuronal circuit reconstruction. *Current Opinion in Neurobiology*, *22*(1), 154–161. https://doi.org/10.1016/J.CONB.2011.10.022

Caers, J., Verlinden, H., Zels, S., Vandersmissen, H. P., Vuerinckx, K., & Schoofs, L. (2012). More than two decades of research on insect neuropeptide GPCRs: An overview. *Frontiers in Endocrinology*, *3*(NOV), 37713. https://doi.org/10.3389/FENDO.2012.00151/BIBTEX

Cardona, A., Saalfeld, S., Schindelin, J., Arganda-Carreras, I., Preibisch, S., Longair, M., Tomancak, P., Hartenstein, V., & Douglas, R. J. (2012). TrakEM2 Software for Neural Circuit Reconstruction. *PLOS ONE*, *7*(6), e38011. https://doi.org/10.1371/JOURNAL.PONE.0038011

Chang, Y. J., Burton, T., Ha, L., Huang, Z., Olajubelo, A., & Li, C. (2015a). Modulation of Locomotion and Reproduction by FLP Neuropeptides in the Nematode *Caenorhabditis elegans*. *PLOS ONE*, *10*(9), e0135164. https://doi.org/10.1371/JOURNAL.PONE.0135164

Chang, Y. J., Burton, T., Ha, L., Huang, Z., Olajubelo, A., & Li, C. (2015b). Modulation of Locomotion and Reproduction by FLP Neuropeptides in the Nematode *Caenorhabditis elegans*. *PLOS ONE*, *10*(9), e0135164. https://doi.org/10.1371/JOURNAL.PONE.0135164

Chase, D. L., & Koelle, M. R. (2007, February 20). *Biogenic amine neurotransmitters in C. elegans*. WormBook.

Choi, S., Taylor, K. P., Chatzigeorgiou, M., Hu, Z., Schafer, W. R., & Kaplan, J. M. (2015). Sensory Neurons Arouse *C. elegans* Locomotion via Both Glutamate and Neuropeptide Release. *PLOS Genetics*, *11*(7), e1005359. https://doi.org/10.1371/JOURNAL.PGEN.1005359

Civelli, O., Reinscheid, R. K., Zhang, Y., Wang, Z., Fredriksson, R., & Schiöth, H. B. (2013). G Protein–Coupled Receptor Deorphanizations. *Https://Doi.Org/10.1146/Annurev-Pharmtox-010611-134548*, *53*, 127–146. https://doi.org/10.1146/ANNUREV-PHARMTOX-010611-134548

Cook, S. J., Crouse, C. M., Yemini, E., Hall, D. H., Emmons, S. W., & Hobert, O. (2020). The connectome of the *Caenorhabditis elegans* pharynx. *The Journal of Comparative Neurology*, *528*(16), 2767. https://doi.org/10.1002/CNE.24932

Cook, S. J., Jarrell, T. A., Brittin, C. A., Wang, Y., Bloniarz, A. E., Yakovlev, M. A., Nguyen, K. C. Q., Tang, L. T.-H., Bayer, E. A., Duerr, J. S., Bülow, H. E., Hobert, O., Hall, D. H., & Emmons, S. W. (2019). Whole-animal connectomes of both Caenorhabditis elegans sexes. *Nature*, *571*(7763), 63–71. https://doi.org/10.1038/s41586-019-1352-7

de Wied, D., & van Ree, J. M. (1989). Neuropeptides: Animal behaviour and human psychopathology. *European Archives of Psychiatry and Neurological Sciences*, *238*(5–6), 323–331. https://doi.org/10.1007/BF00449813/METRICS

Discovery and analysis of the C. elegans Neuronal Gene Expression Network -- CeNGEN. (n.d.). Retrieved June 10, 2024, from https://cengen.shinyapps.io/CengenApp/

Fleur L Strand. (1998, December 8). *Neuropeptides: Regulators of Physiological Processes*. The MIT Press. https://mitpress.mit.edu/9780262194075/neuropeptides/

Frooninckx, L., Van Rompay, L., Temmerman, L., Van Sinay, E., Beets, I., Janssen, T., Husson, S., & Schoofs, L. (2012). Neuropeptide GPCRs in *C. elegans*. *Frontiers in Endocrinology*, *3*. https://www.frontiersin.org/articles/10.3389/fendo.2012.00167

Fujiwara, M., Sengupta, P., & McIntire, S. L. (2002). Regulation of Body Size and Behavioral State of *C. elegans* by Sensory Perception and the EGL-4 cGMP-Dependent Protein Kinase. *Neuron*, *36*(6), 1091–1102. https://doi.org/10.1016/S0896-6273(02)01093-0

Fuxe, K., Borroto-Escuela, D. O., Romero-Fernandez, W., Ciruela, F., Manger, P., Leo, G., Díaz-Cabiale, Z., & Agnati, L. F. (2012). On the role of volume transmission and receptor–receptor interactions in social behaviour: Focus on central catecholamine and oxytocin neurons. *Brain Research*, *1476*, 119–131. https://doi.org/10.1016/J.BRAINRES.2012.01.062

Galili, D. S., Jefferis, G. S., & Costa, M. (2022). Connectomics and the neural basis of behaviour. *Current Opinion in Insect Science*, *54*, 100968. https://doi.org/10.1016/J.COIS.2022.100968

Garriga, G., Desai, C., & Robert Horvitz, H. (1993). Cell interactions control the direction of outgrowth, branching and fasciculation of the HSN axons of *Caenorhabditis elegans*. *Development*, *117*(3), 1071–1087. https://doi.org/10.1242/DEV.117.3.1071

Ge, M. H., Wang, W., Wu, T. H., Wen, X., Al-Sheikh, U., Chen, L. L., Yin, S. W., Wu, J. J., Huang, J. H., He, Q. Q., Liu, H., Li, R., Wang, P. Z., & Wu, Z. X. (2020). Dual Recombining-out System for Spatiotemporal Gene Expression in *C. elegans*. *IScience*, *23*(10), 101567. https://doi.org/10.1016/J.ISCI.2020.101567

Gray, J. M., Karow, D. S., Lu, H., Chang, A. J., Chang, J. S., Ellis, R. E., Marietta, M. A., & Bargmann, C. I. (2004). Oxygen sensation and social feeding mediated by a *C. elegans* guanylate cyclase homologue. *Nature*, *430*(6997), 317–322. https://doi.org/10.1038/NATURE02714

Green, M. R., & Sambrook, J. (2012). Molecular Cloning: A Laboratory Manual (Fourth Edition). In *CSHL Press* (Vol. 1). CSHL press. https://cshlpress.com/default.tpl?action=full&src=pdf&--eqskudatarq=934

Hall, D. H., Lints, R., & Altun, Z. (2005). Nematode Neurons: Anatomy and Anatomical Methods in *Caenorhabditis elegans*. *International Review of Neurobiology*, *69*, 1–35. https://doi.org/10.1016/S0074-7742(05)69001-0

Hammarlund, M., Watanabe, S., Schuske, K., & Jorgensen, E. M. (2008). CAPS and syntaxin dock dense core vesicles to the plasma membrane in neurons. *Journal of Cell Biology*, *180*(3), 483–491. https://doi.org/10.1083/JCB.200708018

Hardaker, L. A., Singer, E., Kerr, R., Zhou, G., & Schafer, W. R. (2001). Serotonin modulates locomotory behavior and coordinates egg-laying and movement in *Caenorhabditis elegans*. *Journal of Neurobiology*, *49*(4), 303–313. https://doi.org/10.1002/NEU.10014

He, S., Cuentas-Condori, A., & Miller, D. M. (2019). NATF (Native and Tissue-Specific Fluorescence): A Strategy for Bright, Tissue-Specific GFP Labeling of Native Proteins in *Caenorhabditis elegans*. *Genetics*, *212*(2), 387. https://doi.org/10.1534/GENETICS.119.302063

Heinrichs, M., & Domes, G. (2008). Neuropeptides and social behaviour: effects of oxytocin and vasopressin in humans. *Progress in Brain Research*, *170*, 337–350. https://doi.org/10.1016/S0079-6123(08)00428-7

Hostettler, L., Grundy, L., Käser-Pébernard, S., Wicky, C., Schafer, W. R., & Glauser, D. A. (2017). The bright fluorescent protein mNeonGreen facilitates protein expression analysis in vivo. *G3: Genes, Genomes, Genetics*, *7*(2), 607–615. https://doi.org/10.1534/G3.116.038133/-/DC1

Husson, S. J., Clynen, E., Baggerman, G., Janssen, T., & Schoofs, L. (2006). Defective processing of neuropeptide precursors in *Caenorhabditis elegans* lacking proprotein convertase 2 (KPC-2/EGL-3): mutant analysis by mass spectrometry. *Journal of Neurochemistry*, *98*(6), 1999–2012. https://doi.org/10.1111/J.1471-4159.2006.04014.X

Izquierdo, E. J., & Beer, R. D. (2018). From head to tail: a neuromechanical model of forward locomotion in *Caenorhabditis elegans*. *Philosophical Transactions of the Royal Society B: Biological Sciences*, *373*(1758). https://doi.org/10.1098/RSTB.2017.0374

Jacob, T. C., & Kaplan, J. M. (2003). The EGL-21 Carboxypeptidase E Facilitates Acetylcholine Release at *Caenorhabditis elegans* Neuromuscular Junctions. *Journal of Neuroscience*, *23*(6), 2122–2130. https://doi.org/10.1523/JNEUROSCI.23-06-02122.2003

Jan, L. Y., & Jan, Y. N. (1982). Peptidergic transmission in sympathetic ganglia of the frog. *The Journal of Physiology*, *327*(1), 219–246. https://doi.org/10.1113/JPHYSIOL.1982.SP014228

Jarrell, T. A., Wang, Y., Bloniarz, A. E., Brittin, C. A., Xu, M., Thomson, J. N., Albertson, D. G., Hall, D. H., & Emmons, S. W. (2012). The Connectome of a Decision-Making Neural Network. *Science*, *337*(6093), 437–444. https://doi.org/10.1126/science.1221762

Javer, A., Ripoll-Sánchez, L., & Brown, A. E. X. (2018). Powerful and interpretable behavioural features for quantitative phenotyping of *Caenorhabditis elegans*. *Philosophical Transactions of the Royal Society B: Biological Sciences*, *373*(1758). https://doi.org/10.1098/RSTB.2017.0375

Jékely, G., Melzer, S., Beets, I., Kadow, I. C. G., Koene, J., Haddad, S., & Holden-Dye, L. (2018). The long and the short of it -A perspective on peptidergic regulation of circuits and behaviour. *Journal of Experimental Biology*, *221*(3). https://doi.org/10.1242/JEB.166710/20346

Kadandale, P., Chatterjee, I., & Singson, A. (2009). Germline transformation of *Caenorhabditis elegans* by injection. *Methods in Molecular Biology (Clifton, N.J.)*, *518*, 123. https://doi.org/10.1007/978-1-59745-202-1_10

Karhunen, T., Vilim, F. S., Alexeeva, V., Weiss, K. R., & Church, P. J. (2001). Targeting of peptidergic vesicles in cotransmitting terminals. *The Journal of Neuroscience : The Official Journal of the Society for Neuroscience*, *21*(3). https://doi.org/10.1523/JNEUROSCI.21-03-J0005.2001

Kass, J., Jacob, T. C., Kim, P., & Kaplan, J. M. (2001). The EGL-3 Proprotein Convertase Regulates Mechanosensory Responses of *Caenorhabditis elegans*. *Journal of Neuroscience*, *21*(23), 9265–9272. https://doi.org/10.1523/JNEUROSCI.21-23-09265.2001

Kawano, T., Ito, Y., Ishiguro, M., Takuwa, K., Nakajima, T., & Kimura, Y. (2000). Molecular cloning and characterization of a new insulin/IGF-like peptide of the

nematode *Caenorhabditis elegans*. *Biochemical and Biophysical Research Communications*, *273*(2), 431–436. https://doi.org/10.1006/BBRC.2000.2971

Lee, S. H., & Dan, Y. (2012a). Neuromodulation of Brain States. *Neuron*, *76*(1), 209–222. https://doi.org/10.1016/J.NEURON.2012.09.012

Lee, S. H., & Dan, Y. (2012b). Neuromodulation of Brain States. *Neuron*, *76*(1), 209–222. https://doi.org/10.1016/J.NEURON.2012.09.012

Li, C., & Kim, K. (2008, September 25). *Neuropeptides*. WormBook.

Li, C., Nelson, L. S., Kim, K., Nathoo, A., & Hart, A. C. (1999). Neuropeptide gene families in the nematode *Caenorhabditis elegans*. *Annals of the New York Academy of Sciences*, *897*, 239–252. https://doi.org/10.1111/J.1749-6632.1999.TB07895.X

Lim, M. A., Chitturi, J., Laskova, V., Meng, J., Findeis, D., Wiekenberg, A., Mulcahy, B., Luo, L., Li, Y., Lu, Y., Hung, W., Qu, Y., Ho, C. Y., Holmyard, D., Ji, N., McWhirter, R., Samuel, A. D. T., Miller, D. M., Schnabel, R., … Zhen, M. (2016). Neuroendocrine modulation sustains the *C. elegans* forward motor state. *ELife*, *5*(NOVEMBER2016). https://doi.org/10.7554/ELIFE.19887

Liu, Q., Liu, S., Kodama, L., Driscoll, M. R., & Wu, M. N. (2012). Two Dopaminergic Neurons Signal to the Dorsal Fan-Shaped Body to Promote Wakefulness in *Drosophila*. *Current Biology*, *22*(22), 2114–2123. https://doi.org/10.1016/J.CUB.2012.09.008

Lu, Y., Ahamed, T., Mulcahy, B., Meng, J., Witvliet, D., Guan, S. A., Holmyard, D., Hung, W., Wen, Q., Chisholm, A. D., Samuel, A. D. T., & Zhen, M. (2022). Extrasynaptic signaling enables an asymmetric juvenile motor circuit to produce symmetric undulation. *Current Biology : CB*, *32*(21), 4631-4644.e5. https://doi.org/10.1016/J.CUB.2022.09.002

Luigi F. Agnati, Börje Bjelke, & Kjell Fuxe. (1992, July). *Volume Transmission in the Brain*. Sigma Xi, The Scientific Research Honor Society. https://doi.org/https://www.jstor.org/stable/29774687

Mains, R. E., & Eipper, B. A. (1999). *The Neuropeptides*. https://www.ncbi.nlm.nih.gov/books/NBK28247/

Marder, E. (2012a). Neuromodulation of Neuronal Circuits: Back to the Future. *Neuron*, *76*(1), 1–11. https://doi.org/10.1016/J.NEURON.2012.09.010

Marder, E. (2012b). Neuromodulation of Neuronal Circuits: Back to the Future. *Neuron*, *76*(1), 1–11. https://doi.org/10.1016/J.NEURON.2012.09.010

Marder, E., & Bucher, D. (2007). Understanding circuit dynamics using the stomatogastric nervous system of lobsters and crabs. *Annual Review of Physiology*, *69*, 291–316. https://doi.org/10.1146/ANNUREV.PHYSIOL.69.031905.161516

Marquina-Solis, J., Vandewyer, E., Hawk, J., Colón-Ramos, D. A., Beets, I., & Bargmann, C. I. (2022). Peptidergic signaling controls the dynamics of sickness behavior in *Caenorhabditis elegans*; *BioRxiv*, 2022.04.16.488560. https://doi.org/10.1101/2022.04.16.488560

McKay, F. M., McCoy, C. J., Crooks, B., Marks, N. J., Maule, A. G., Atkinson, L. E., & Mousley, A. (2022). In silico analyses of neuropeptide-like protein (NLP) profiles in parasitic nematodes. *International Journal for Parasitology*, *52*(1), 77–85. https://doi.org/https://doi.org/10.1016/j.ijpara.2021.07.002

Mirabeau, O., & Joly, J. S. (2013). Molecular evolution of peptidergic signaling systems in bilaterians. *Proceedings of the National Academy of Sciences of the United States of America*, *110*(22), E2028–E2037. https://doi.org/10.1073/PNAS.1219956110/SUPPL_FILE/SD01.PDF

Motomura, H., Ioroi, M., Murakami, K., Kuhara, A., & Ohta, A. (2022). Head-tail-head neural wiring underlies gut fat storage in *Caenorhabditis elegans* temperature acclimation. *Proceedings of the National Academy of Sciences of the United States of America*, *119*(32), e2203121119. https://doi.org/10.1073/PNAS.2203121119/SUPPL_FILE/PNAS.2203121119.SD02.XLSX

Mulcahy, B., Witvliet, D., Holmyard, D., Mitchell, J., Chisholm, A. D., Samuel, A. D. T., & Zhen, M. (2018). A pipeline for volume electron microscopy of the *caenorhabditis elegans* nervous system. *Frontiers in Neural Circuits*, *12*, 419735. https://doi.org/10.3389/FNCIR.2018.00094/BIBTEX

Nässel, D. R. (2009). Neuropeptide signaling near and far: how localized and timed is the action of neuropeptides in brain circuits? *Invertebrate Neuroscience 2009 9:2*, *9*(2), 57–75. https://doi.org/10.1007/S10158-009-0090-1

Nelson, L. S., Kim, K., Memmott, J. E., & Li, C. (1998). FMRFamide-related gene family in the nematode, *Caenorhabditis elegans*. *Brain Research. Molecular Brain Research*, *58*(1–2), 103–111. https://doi.org/10.1016/S0169-328X(98)00106-5

Niu, L., Li, Y., Zong, P., Liu, P., Shui, Y., Chen, B., & Wang, Z. W. (2020). Melatonin promotes sleep by activating the BK channel in *C. elegans*. *Proceedings of the National Academy of Sciences of the United States of America*, *117*(40), 25128–25137.

https://doi.org/10.1073/PNAS.2010928117/SUPPL_FILE/PNAS.2010928117.SAPP.PDF

Nusbaum, M. P. (2002). Regulating Peptidergic Modulation of Rhythmically Active Neural Circuits. *Brain Behavior and Evolution*, *60*(6), 378–387. https://doi.org/10.1159/000067791

Ohnuma, K., Whim, M. D., Fetter, R. D., Kaczmarek, L. K., & Zucker, R. S. (2001). Presynaptic target of Ca2+ action on neuropeptide and acetylcholine release in *Aplysia californica*. *The Journal of Physiology*, *535*(Pt 3), 647–662. https://doi.org/10.1111/J.1469-7793.2001.00647.X

Oranth, A., Schultheis, C., Tolstenkov, O., Erbguth, K., Nagpal, J., Hain, D., Brauner, M., Wabnig, S., Steuer Costa, W., McWhirter, R. D., Zels, S., Palumbos, S., Miller, D. M., Beets, I., & Gottschalk, A. (2018). Food Sensation Modulates Locomotion by Dopamine and Neuropeptide Signaling in a Distributed Neuronal Network. *Neuron*, *100*(6), 1414-1428.e10. https://doi.org/10.1016/J.NEURON.2018.10.024

Pereira, L., Kratsios, P., Serrano-Saiz, E., Sheftel, H., Mayo, A. E., Hall, D. H., White, J. G., LeBoeuf, B., Garcia, L. R., Alon, U., & Hobert, O. (2015). A cellular and regulatory map of the cholinergic nervous system of *C. Elegans*. *ELife*, *4*(DECEMBER2015). https://doi.org/10.7554/ELIFE.12432

Randi, F., Sharma, A. K., Dvali, S., & Leifer, A. M. (2023). Neural signal propagation atlas of *Caenorhabditis elegans*. *Nature 2023 623:7986*, *623*(7986), 406–414. https://doi.org/10.1038/s41586-023-06683-4

Ripoll-Sánchez, L., Watteyne, J., Sun, H. S., Fernandez, R., Taylor, S. R., Weinreb, A., Bentley, B. L., Hammarlund, M., Miller, D. M., Hobert, O., Beets, I., Vértes, P. E., & Schafer, W. R. (2023). The neuropeptidergic connectome of *C. elegans*. *Neuron*, *111*(22), 3570-3589.e5. https://doi.org/10.1016/J.NEURON.2023.09.043

Rolls, M. M., Hall, D. H., Victor, M., Stelzer, E. H. K., & Rapoport, T. A. (2002). Targeting of rough endoplasmic reticulum membrane proteins and ribosomes in invertebrate neurons. *Molecular Biology of the Cell*, *13*(5), 1778–1791. https://doi.org/10.1091/MBC.01-10-0514/ASSET/IMAGES/LARGE/MK0521835007.JPEG

Rostaing, P., Weimer, R. M., Jorgensen, E. M., Triller, A., & Bessereau, J. L. (2004). Preservation of Immunoreactivity and Fine Structure of Adult *C. elegans* Tissues Using High-pressure Freezing. *Journal of Histochemistry and Cytochemistry*, *52*(1), 1–12. https://doi.org/10.1177/002215540405200101/ASSET/IMAGES/LARGE/10.1177_002215540405200101-FIG7.JPEG

Rudolf, R., Salm, T., Rustom, A., & Gerdes, H. H. (2001). Dynamics of immature secretory granules: Role of cytoskeletal elements during transport, cortical restriction, and F-actin-dependent tethering. *Molecular Biology of the Cell*, *12*(5), 1353–1365. https://doi.org/10.1091/MBC.12.5.1353/ASSET/IMAGES/LARGE/MK0511482007.JPEG

Saalfeld, S., Cardona, A., Hartenstein, V., & Tomančák, P. (2009a). CATMAID: collaborative annotation toolkit for massive amounts of image data. *Bioinformatics*, *25*(15), 1984–1986. https://doi.org/10.1093/BIOINFORMATICS/BTP266

Saalfeld, S., Cardona, A., Hartenstein, V., & Tomančák, P. (2009b). CATMAID: collaborative annotation toolkit for massive amounts of image data. *Bioinformatics*, *25*(15), 1984–1986. https://doi.org/10.1093/BIOINFORMATICS/BTP266

Salio, C., Lossi, L., Ferrini, F., & Merighi, A. (2006). Neuropeptides as synaptic transmitters. *Cell and Tissue Research*, *326*(2), 583–598. https://doi.org/10.1007/S00441-006-0268-3

Shaner, N. C., Lambert, G. G., Chammas, A., Ni, Y., Cranfill, P. J., Baird, M. A., Sell, B. R., Allen, J. R., Day, R. N., Israelsson, M., Davidson, M. W., & Wang, J. (2013). A bright monomeric green fluorescent protein derived from *Branchiostoma lanceolatum. Nature Methods 2013 10:5*, *10*(5), 407–409. https://doi.org/10.1038/nmeth.2413

Stiernagle, T. (2006). Maintenance of *C. elegans*. *WormBook : The Online Review of C. Elegans Biology*, 1–11. https://doi.org/10.1895/WORMBOOK.1.101.1

Strand, F. L. (1999). *Neuropeptides : regulators of physiological processes*. 658. https://mitpress.mit.edu/9780262194075/neuropeptides/

Subramaniam, S. (2005). Bridging the imaging gap: visualizing subcellular architecture with electron tomography. *Current Opinion in Microbiology*, *8*(3), 316. https://doi.org/10.1016/J.MIB.2005.04.012

Sulston, J. E., & Horvitz, H. R. (1977). Post-embryonic cell lineages of the nematode, *Caenorhabditis elegans*. *Developmental Biology*, *56*(1), 110–156. https://doi.org/10.1016/0012-1606(77)90158-0

Sun, H., & Hobert, O. (2023). Temporal transitions in the postembryonic nervous system of the nematode *Caenorhabditis elegans*: Recent insights and open questions. *Seminars in Cell & Developmental Biology*, *142*, 67–80. https://doi.org/10.1016/J.SEMCDB.2022.05.029

Sun, H. S., & Hobert, O. (2021). Temporal transitions in the post-mitotic nervous system of *Caenorhabditis elegans*. *Nature 2021 600:7887*, *600*(7887), 93–99. https://doi.org/10.1038/s41586-021-04071-4

Swallow, J. G., Bubak, A. N., & Grace, J. L. (2016). The role of monoamines in modulating behavior. *Current Zoology*, *62*(3), 253. https://doi.org/10.1093/CZ/ZOW046

Taylor, S. R., Santpere, G., Weinreb, A., Barrett, A., Reilly, M. B., Xu, C., Varol, E., Oikonomou, P., Glenwinkel, L., McWhirter, R., Poff, A., Basavaraju, M., Rafi, I., Yemini, E., Cook, S. J., Abrams, A., Vidal, B., Cros, C., Tavazoie, S., … Miller, D. M. (2021a). Molecular topography of an entire nervous system. *Cell*, *184*(16), 4329-4347.e23. https://doi.org/10.1016/J.CELL.2021.06.023

Taylor, S. R., Santpere, G., Weinreb, A., Barrett, A., Reilly, M. B., Xu, C., Varol, E., Oikonomou, P., Glenwinkel, L., McWhirter, R., Poff, A., Basavaraju, M., Rafi, I., Yemini, E., Cook, S. J., Abrams, A., Vidal, B., Cros, C., Tavazoie, S., … Miller, D. M. (2021b). Molecular topography of an entire nervous system. *Cell*, *184*(16), 4329-4347.e23. https://doi.org/10.1016/J.CELL.2021.06.023

Trueta, C., & De-Miguel, F. F. (2012a). Extrasynaptic exocytosis and its mechanisms: A source of molecules mediating volume transmission in the nervous system. *Frontiers in Physiology*, *3 SEP*, 27664. https://doi.org/10.3389/FPHYS.2012.00319/BIBTEX

Trueta, C., & De-Miguel, F. F. (2012b). Extrasynaptic exocytosis and its mechanisms: A source of molecules mediating volume transmission in the nervous system. *Frontiers in Physiology*, *3 SEP*. https://doi.org/10.3389/fphys.2012.00319

Tsukita, S., & Ishikawa, H. (1980). The movement of membranous organelles in axons. Electron microscopic identification of anterogradely and retrogradely transported organelles. *Journal of Cell Biology*, *84*(3), 513–530. https://doi.org/10.1083/JCB.84.3.513

Turek, M., Besseling, J., Spies, J. P., König, S., & Bringmann, H. (2016). Sleep-active neuron specification and sleep induction require FLP-11 neuropeptides to systemically induce sleep. *ELife*, *5*(MARCH2016). https://doi.org/10.7554/ELIFE.12499

Valperga, G., & de Bono, M. (2022). Impairing one sensory modality enhances another by reconfiguring peptidergic signalling in *Caenorhabditis elegans*. *ELife*, *11*. https://doi.org/10.7554/ELIFE.68040

Van Bael, S., Zels, S., Boonen, K., Beets, I., Schoofs, L., & Temmerman, L. (2018). A *Caenorhabditis elegans* Mass Spectrometric Resource for Neuropeptidomics.

Journal of the American Society for Mass Spectrometry, *29*(5), 879–889. https://doi.org/10.1007/S13361-017-1856-Z

Van Damme, S., De Fruyt, N., Watteyne, J., Kenis, S., Peymen, K., Schoofs, L., & Beets, I. (2021). Neuromodulatory pathways in learning and memory: Lessons from invertebrates. *Journal of Neuroendocrinology*, *33*(1), e12911. https://doi.org/10.1111/JNE.12911

Vogt, K. (2020). Towards a functional connectome in Drosophila. *Journal of Neurogenetics*, *34*(1), 156–161. https://doi.org/10.1080/01677063.2020.1712598

Walker, R. J., Brooks, H. L., & Holden-Dye, L. (1996). Evolution and overview of classical transmitter molecules and their receptors. *Parasitology*, *113*(S1), S3–S33. https://doi.org/10.1017/S0031182000077878

Wang, C., Vidal, B., Sural, S., Merritt, D. M., Toker, I. A., Vogt, M. C., Cros, C., & Hobert, O. (2024a). A neurotransmitter atlas of the nervous system of *C. elegans* males and hermaphrodites. *ELife*, *13*. https://doi.org/10.7554/ELIFE.95402.1

Wang, C., Vidal, B., Sural, S., Merritt, D. M., Toker, I. A., Vogt, M. C., Cros, C., & Hobert, O. (2024b). A neurotransmitter atlas of the nervous system of *C. elegans* males and hermaphrodites. *ELife*, *13*. https://doi.org/10.7554/ELIFE.95402.1

Watteyne, J., Peymen, K., Van der Auwera, P., Borghgraef, C., Vandewyer, E., Van Damme, S., Rutten, I., Lammertyn, J., Jelier, R., Schoofs, L., & Beets, I. (2020). Neuromedin U signaling regulates retrieval of learned salt avoidance in a C. elegans gustatory circuit. *Nature Communications 2020 11:1*, *11*(1), 1–16. https://doi.org/10.1038/s41467-020-15964-9

Wen, Q., Po, M. D., Hulme, E., Chen, S., Liu, X., Kwok, S. W., Gershow, M., Leifer, A. M., Butler, V., Fang-Yen, C., Kawano, T., Schafer, W. R., Whitesides, G., Wyart, M., Chklovskii, D. B., Zhen, M., & Samuel, A. D. T. (2012a). Proprioceptive Coupling within Motor Neurons Drives *C. elegans* Forward Locomotion. *Neuron*, *76*(4), 750–761. https://doi.org/10.1016/j.neuron.2012.08.039

Wen, Q., Po, M. D., Hulme, E., Chen, S., Liu, X., Kwok, S. W., Gershow, M., Leifer, A. M., Butler, V., Fang-Yen, C., Kawano, T., Schafer, W. R., Whitesides, G., Wyart, M., Chklovskii, D. B., Zhen, M., & Samuel, A. D. T. (2012b). Proprioceptive Coupling within Motor Neurons Drives *C. elegans* Forward Locomotion. *Neuron*, *76*(4), 750–761. https://doi.org/10.1016/j.neuron.2012.08.039

White, J. G., Southgate, E., Thomson, J. N., & Brenner, S. (1986a). The Structure of the Nervous System of the Nematode *Caenorhabditis elegans*. In *Philosophical Transactions of the Royal Society of London. Series B, Biological Sciences* (Vol. 314).

http://www.jstor.orgURL:http://www.jstor.org/stable/2990196Accessed:24/07/200815:13

White, J. G., Southgate, E., Thomson, J. N., & Brenner, S. (1986b). The Structure of the Nervous System of the Nematode *Caenorhabditis elegans*. In *Philosophical Transactions of the Royal Society of London. Series B, Biological Sciences* (Vol. 314). http://www.jstor.orgURL:http://www.jstor.org/stable/2990196Accessed:24/07/200815:13

Witvliet, D., Mulcahy, B., Mitchell, J. K., Meirovitch, Y., Berger, D. R., Wu, Y., Liu, Y., Koh, W. X., Parvathala, R., Holmyard, D., Schalek, R. L., Shavit, N., Chisholm, A. D., Lichtman, J. W., Samuel, A. D. T., & Zhen, M. (2021). Connectomes across development reveal principles of brain maturation. *Nature 2021 596:7871*, *596*(7871), 257–261. https://doi.org/10.1038/s41586-021-03778-8

Xu, M., Jarrell, T. A., Wang, Y., Cook, S. J., Hall, D. H., & Emmons, S. W. (2013). Computer Assisted Assembly of Connectomes from Electron Micrographs: Application to *Caenorhabditis elegans*. *PLOS ONE*, *8*(1), e54050. https://doi.org/10.1371/JOURNAL.PONE.0054050

Xu, Y., Zhang, L., Liu, Y., Topalidou, I., Hassinan, C., Ailion, M., Zhao, Z., Wang, T., Chen, Z., & Bai, J. (2021). Dopamine receptor DOP-1 engages a sleep pathway to modulate swimming in *C. elegans*. *IScience*, *24*(4), 102247. https://doi.org/10.1016/J.ISCI.2021.102247

Yang, K., Liu, T., Liu, H., Di, Z., & Zhang, K. (2021). Ultrastructural features of presynaptic active zones and dense core vesicles of olfactory projection neuron boutons in *Drosophila melanogaster*. *BioRxiv*, 2021.01.12.426300. https://doi.org/10.1101/2021.01.12.426300

Ye, C., Xu, S., Hu, Q., Zhou, L., Qin, X., Jia, J., & Hu, G. (2019). Global view of neuropeptides and their receptors in the brain and pituitary of grass carp (Ctenopharyngodon idellus). *Aquaculture*, *512*, 734360. https://doi.org/10.1016/J.AQUACULTURE.2019.734360

Zimmer, M., Gray, J. M., Pokala, N., Chang, A. J., Karow, D. S., Marletta, M. A., Hudson, M. L., Morton, D. B., Chronis, N., & Bargmann, C. I. (2009). Neurons Detect Increases and Decreases in Oxygen Levels Using Distinct Guanylate Cyclases. *Neuron*, *61*(6), 865–879. https://doi.org/10.1016/J.NEURON.2009.02.013

Appendix

1. Risk analysis

1.1. General

These experiments were carried out in s laboratory of biosafety level 1, working with non-pathogenic organisms: *C. elegans* and *E. coli* OP50. While doing the experiments in the laboratory, wearing a lab coat and gloves were necessary. The lab coat was not to be used in areas with food and/or drinks. Additionally, food, drinks, and smoking were prohibited in the lab. Hands should be washed with soap and water when leaving the lab. When using the laminar air flow hood, the gloves, and materials to be used were disinfected with 70% alcohol. Waste generated had to be sorted into the appropriate containers. Solid biohazardous waste was to be disposed in the yellow waste cardboard box with the yellow plastic bag inside. Any sharp objects to be discarded, such as needles, were disposed in the designated containers.

1.2. Products

1.2.1. GelRed

To stain DNA during gel electrophoresis, GelRed is used. However, its risks are not fully understood, so physical contact must always be avoided. No materials from the gel electrophoresis room can be removed. A lab coat with a red collar and gloves are designated for use in this room.

1.2.2. $CaCl_2$

$CaCl_2$ can be an irritant to the eyes, so eye and face protection are required. If contact occurs, rinse with water for several minutes.

1.2.3. EtOH

Ethanol is highly flammable and can cause eye irritation. It should be stored in a closed container away from heat.

2. Solutions and Buffers

2.1. 1M MgSO4

To prepare 200mL of 1M $MgSO_4$ solution, dissolve 49.3g $MgSO_4$ (246.5g/mol) in Milli Q water up to 200mL in a 500mL Duran bottle. Swirl gently to homogenize and autoclave. Under laminar flow, aliquot into 50mL Falcon tubes.

2.2. 1M CaCl2

To prepare 200mL of 1M $CaCl_2$ solution, dissolve 147g $CaCl_2$ (147.01g/mol) in Milli Q water up to 200mL in a 500mL Duran bottle. Swirl gently to homogenize and autoclave. Under laminar flow, aliquot into 50mL Falcon tubes.

2.3. 5mg/mL Cholesterol

To prepare 200mL of 5mg/mL cholesterol solution, dissolve 1g cholesterol (386.65g/mol) in 100% EtOH up to 200mL in a 500mL Duran bottle. Swirl gently to homogenize and autoclave. Under laminar flow, aliquot into 50mL Falcon tubes.

2.4. 1M P Buffer

To prepare 200mL of 1M P buffer, dissolve 21.77g KH_2PO_4 (136.09g/mol) and 6.97g K_2HPO_4 (174.18g/mol) in Milli Q water up to 200mL in a 500mL Duran bottle. Swirl gently to homogenize and autoclave.

2.5. 2xTY Medium Broth

To prepare 200mL of 2xTY medium broth, dissolve 3.2g Bactotryptone, 2g yeast extract, and 1g NaCl (58.44g/mol) in Milli Q water up to 200mL in a 500mL Duran bottle. Swirl gently to homogenize and autoclave.

2.6. 50x TAE Buffer

To prepare 1L of 50x TAE buffer, dissolve 242g Trizma base (121.14g/mol) and 18.61g disodium EDTA (372.24g/mol) in 700mL AD water in a plastic bottle. Stir until dissolved, then add 57.1mL acetic acid (60.05g/mol) and swirl gently to homogenize. Add AD water up to 1L.

2.7. Bleach solution (1mL)

To prepare 1mL of bleach solution, mix 500µL 1M NaOH with 500µL household bleach (5% sodium hypochlorite).

2.8. PCR Template Buffer

To prepare 100mL of PCR template buffer, mix:

- 1mL of 1% gelatin
- 5mL of KCl
- 0.25mL of 1M $MgCl_2$
- 1mL of 1M Tris in HCl (pH 8.3)
- 4.5mL of 10% NP-40
- 4.5mL of 10% Tween 20

2.9. S Basal

To prepare 200mL of S basal, dissolve 1.17g NaCl, 1.2g KH_2PO_4, and 0.2g K_2HPO_4 in Milli Q water up to 200mL in a 500mL Duran bottle. Swirl gently to homogenize and autoclave.

3. Plasmids

The plasmid pJH4237 was a gift from Mei Zhen (Addgene plasmid # 191538; http://n2t.net/addgene:191538; RRID: Addgene_191538). It was used to express Cre recombinase in a cell-type specific manner.

pJH4237	Ptwk-40s::Cre unc-54 3' UTR for Cre/Lox	*C. elegans*	Addgene plasmid # 191538

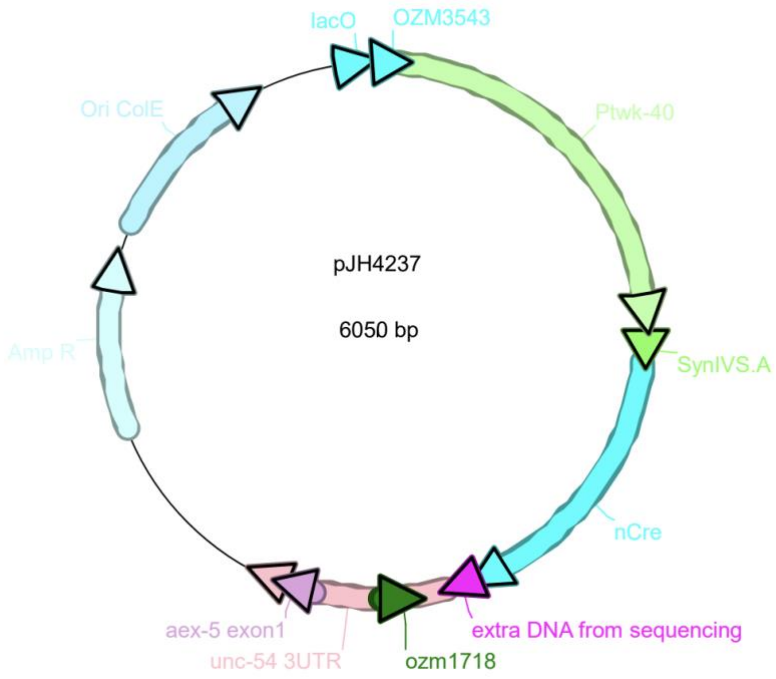

Figure 17: The genetic map of plasmid pJH4237 (Lu et al., 2022)**.** This plasmid is utilized to express Cre recombinase in a cell type-specific manner. The promoter sequence Ptwk-40 is flanked by restriction sites, allowing for its removal and replacement with a promoter of interest. (Ptwk-40: promoter sequence of the twk-40 gene, nCre: Cre recombinase, AmpR: Ampicillin resistance gene).

4. Promoter sequence for *nlp-17.*

The DNA sequence for the promoter of *nlp-17* gene (298bp) was obtained from the Frøkjær-Jensen Lab (AlHarbi & Frøkjær-Jensen, 2023).

WormBase ID	Gene name	Promoter sequence (modifications in upper case, consensus start site in bold)
WBGene00003755	*nlp-17*	actttgatgtttcaaaagttttcctaatctatatgttttttcgcagcctatt atctcaaaaacttattatttatttatttatctaggttattacgggaatggat gagggggtgacgtttttgagtttttgagtcgcacttaattagaaaagctata taataactctagatataattactcgActcacttaatagccttgatagctcgc tataattgaaatataaatagtgagatgagccatttaaatcgacatttcgaga ctttttttctcgcgaaaaagtcaggctttttcacaga <b>aaaaATG

AFDELING
Straat nr bus 0000
3000 LEUVEN, BELGIË
tel. + 32 16 00 00 00
fax + 32 16 00 00 00
www.kuleuven.be